

# Geopolymers and Related Alkali-Activated Materials

John L. Provis and Susan A. Bernal

Department of Materials Science and Engineering, University of Sheffield, Sheffield, S1 3JD, United Kingdom; email: j.provis@sheffield.ac.uk, s.bernal@sheffield.ac.uk

Annu. Rev. Mater. Res. 2014. 44:299–327

First published online as a Review in Advance on February 3, 2014

The *Annual Review of Materials Research* is online at [matsci.annualreviews.org](http://matsci.annualreviews.org)

This article's doi:  
10.1146/annurev-matsci-070813-113515

Copyright © 2014 by Annual Reviews.  
All rights reserved

## Keywords

construction materials, sustainable development, cement, concrete, fly ash, blast furnace slag

## Abstract

The development of new, sustainable, low-CO<sub>2</sub> construction materials is essential if the global construction industry is to reduce the environmental footprint of its activities, which is incurred particularly through the production of Portland cement. One type of non-Portland cement that is attracting particular attention is based on alkali-aluminosilicate chemistry, including the class of binders that have become known as geopolymers. These materials offer technical properties comparable to those of Portland cement, but with a much lower CO<sub>2</sub> footprint and with the potential for performance advantages over traditional cements in certain niche applications. This review discusses the synthesis of alkali-activated binders from blast furnace slag, calcined clay (metakaolin), and fly ash, including analysis of the chemical reaction mechanisms and binder phase assemblages that control the early-age and hardened properties of these materials, in particular initial setting and long-term durability. Perspectives for future research developments are also explored.

## 1. INTRODUCTION

### Concrete:

a composite material consisting of coarse and fine mineral particulates (aggregates) bound together with a continuous binder phase to form a hardened product

### Portland cement:

a hydraulic binder produced by calcination of limestone and siliceous matter; consists mainly of calcium silicate phases, with some aluminate/ferrite phases, interground with gypsum

Cement and concrete are central to modern civilization, with its reliance on the built environment to provide a high quality of life. Concrete is the second-most-used commodity in the world behind only water (1) and is produced in volumes exceeding 10 billion tonnes per year worldwide. The binding phase that provides strength to a modern concrete is usually based on Portland cement (2). Portland cement is regarded by society as a low-tech material but is in fact a complex combination of multiple mineral phases that are manufactured to provide years of strength, impermeability, durability, and passivation of embedded carbon steel reinforcement while being subjected to thermal, mechanical, and chemical stresses. These properties are the result of many years of both academic and industrial research and development by chemists, materials scientists, and engineers.

Given its ubiquitous use in civil construction, the very high cement production volume required to generate this enormous quantity of concrete introduces significant environmental issues; cement production (**Figure 1**) contributes ~8% of global CO<sub>2</sub> emissions (3, 4). CO<sub>2</sub> emissions from cement manufacture are mainly due to the thermal decomposition of calcium carbonate to generate the reactive calcium silicate and aluminate phases, the basis of Portland cement. The total emissions footprint of approximately 0.8 tonnes of CO<sub>2</sub> equivalent per tonne of Portland cement produced is divided between emissions from the combustion of fossil fuels and the CO<sub>2</sub> released through the conversion of calcium carbonate to oxide form (5). As global society produces ever-increasing quantities of concrete to meet the infrastructure needs of the developing world (6), there is an urgent need for the development and commercialization of alternative cement-like binders, which

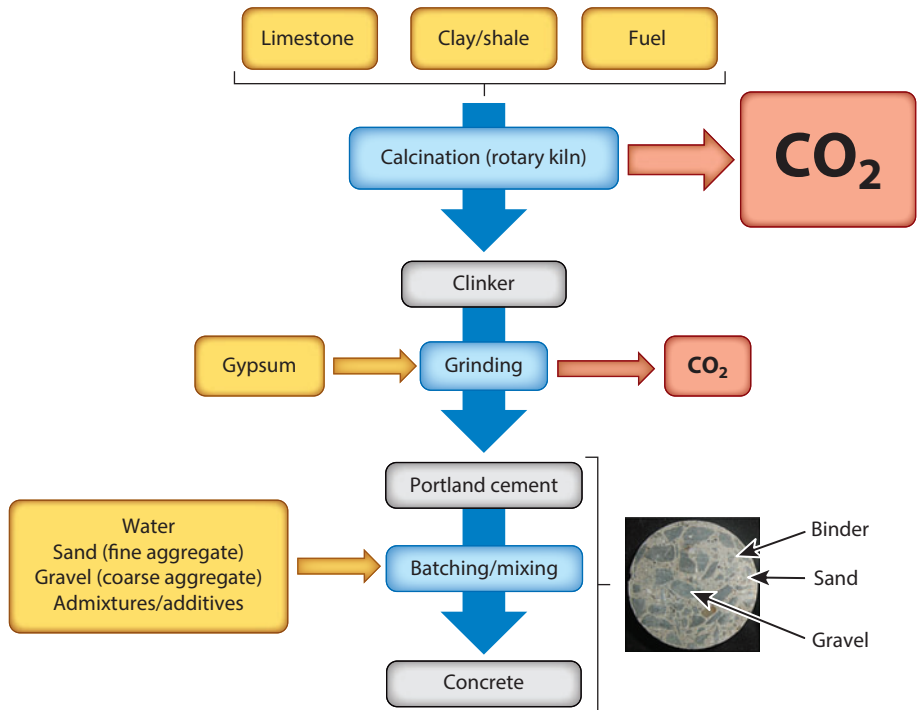


**Figure 1**

Schematic depiction of the process of production of Portland cement concrete.

will enable provision of housing and infrastructure to billions of people without excessive damage to the Earth's atmosphere and seas.

Alkali-activated materials (AAMs) (7), including those classified as geopolymers (8, 9), are a high-profile example of the alternative binders now being discussed and developed with a view toward obtaining environmental savings in the construction industry; others include calcium aluminates, sulfoaluminates, supersulfated slag cements, and magnesium-based binders (10). The main binding phases are derived by the reaction of aluminosilicates sourced from calcined clays, coal fly ash, and/or metallurgical slags, with an alkaline solution that accelerates the reaction process and induces the formation of strong, insoluble binding phases (7). As such, the CO<sub>2</sub> savings achieved by the use of AAM binders are mainly due to the avoidance of carbonate precursors, such as the limestone (CaCO<sub>3</sub>) shown in **Figure 1**, and the high-temperature processing of all the cement constituents in a fossil fuel-fired kiln. This question is revisited in more detail in Section 6.

The main precursors used to produce AAMs are fly ash, blast furnace slag (BFS), and metakaolin. Both fly ash and BFS are in high demand for use in blended Portland cements, which can offer both performance and environmental advantages over a plain Portland cement in applications such as civil infrastructure and general concreting works, and particularly where sulfate resistance is required (13). The question therefore becomes whether it is more efficient to use BFS and fly ash as precursors for AAM production or in blending with Portland cement. Strong arguments for both sides of this discussion exist, and the answer probably lies in finding the optimal balance of utilization: For cements with a relatively high volume of Portland cement, the addition of a moderate amount of fly ash or BFS can be highly beneficial. However, when one is considering very high volume blending (up to 95% replacement of Portland cement by ground BFS is allowed under EN 197-1 for cements in the CEM III/C category), it may be more desirable to utilize a purpose-designed alkaline activator rather than using Portland cement essentially to provide an elevated pH environment to initiate the reaction of the BFS (or fly ash), when the simple provision of alkalinity is not the main purpose for which Portland cement clinker is designed and produced.

Metallurgical slags, particularly BFS, have long been used as cementitious constituents in concretes in Western Europe. Developments in the use of slags in cements date as far back as at least the 1870s in France and Germany (14), and fly ash was first used in concrete in the United States in the 1930s (15). The first modern use of the combination of an alkali with an aluminosilicate to form a cementing binder dates to the early 1900s, when Kühl (16) reported and patented his studies on mixtures of BFS and alkaline components. Purdon published the first extensive laboratory study on cements consisting of slag and alkalis in 1940 (17) and commercialized these materials in Belgium in the 1950s, including constructing several buildings that still stand more than 60 years later (18).

In the mid-1950s, in the context of demand for Portland cement alternatives in the former Soviet Union, Glukhovskiy (19) developed binders using low-calcium or calcium-free aluminosilicate precursors, activated by alkaline solutions containing alkali metals. He termed the binders "soil cements" and the corresponding concretes "soil silicates." These materials have been used in infrastructure, commercial, and domestic construction, on the order of several millions of tonnes, since that time (20). In Northern Europe, alkali-activated slag concretes known as F-concrete were developed and commercialized during the 1980s (21). Cements and concretes produced by alkaline activation of metallurgical slags have been marketed in China for many years (20, 22), motivated by the ability to produce high-strength (>80-MPa) concretes from the high-volume by-products of China's metallurgical industries.

In the 1970s in France, Davidovits (23, 24) developed and began to commercialize alkali-activated binders based on metakaolin. Because the products were sold as a fire-resistant, inorganic resin, he coined the term geopolymer to emphasize some of the similarities in physical properties between these materials and organic thermoset resins. Interest grew in the use of this

---

**Alkali-activated material (AAM):**

a material formed by the reaction between an aluminosilicate precursor and an alkaline activator, with properties comparable to those of a traditional cement binder

**Geopolymer:** an alkali-activated binder material containing little or no calcium; often derived from a metakaolin or a fly ash precursor

**Binder:** the continuous phase (effectively an inorganic glue) in a mortar or concrete; usually hydrated Portland cement, an alkali-activated material, or various other types of cement

**Fly ash:** the solid by-product of coal-fired electricity generation; consists mainly of glassy, spherical aluminosilicate particles

**Blast furnace slag (BFS):** calcium silicate-based product removed from the top of molten iron during its extraction from ore in a blast furnace; usually rapidly cooled to a glassy state and ground for use in construction materials

---



**Figure 2**

Examples of civil construction projects in Australia that have been completed by using E-Crete (alkali-activated) concretes: (a) a residential housing slab, (b) precast external panels, (c) a cast-in-place sidewalk, and (d) a retaining wall surrounding a road bridge. Copyright 2013, Zeobond Pty. Ltd., Docklands, Victoria, Australia (<http://www.zeobond.com>), and reproduced with permission.

**Metakaolin:** the crystallographically disordered layered product of dehydroxylation of kaolinite (an aluminosilicate clay) at a temperature of  $\sim 450\text{--}800^\circ\text{C}$ , below the temperature at which the material recrystallizes to form mullite

type of chemistry as a route to the production of construction materials, and through the 1980s and 1990s, a high-early-strength hybrid Portland/alkali-activated concrete termed Pyrament was marketed in North America (8, 24). Wastiels et al. (25) first described the alkaline activation of fly ash in the early 1990s, and an alkali-activated BFS–fly ash binder was patented and marketed at approximately the same time in the Netherlands as an acid-resistant material for pipe production (26). Ongoing commercialization work in the European Union has also led to commercial production of alkali-activated construction products by companies in the United Kingdom, the Netherlands, the Czech Republic, and increasingly across Europe. Alkali-activated BFS–fly ash blends have been highlighted as a key commercial system in Australia. Such blends have been marketed under the trademark E-Crete and utilized in major civil infrastructure and domestic construction projects (**Figure 2**), including specific descriptions in official regulatory authority specifications for concretes (7, 9).

When used in concrete production, AAMs can provide technical properties that meet almost all performance requirements applied to regular Portland cement–based concretes. Applications can range from nuclear waste immobilization to high-value composite manufacturing to high-volume infrastructure construction (7), which obviously encompasses a highly diverse group of materials.

These materials are grouped under the categories of alkali activated or geopolymeric, where the latter term refers most often to the subset of low-calcium materials (7), as highlighted below. Examples of beneficial properties ascribed to these materials include (27)

- flexural and compressive strength, both early and final;
- high-temperature resistance, including thermal insulating properties;
- stability under chemical (including acid) attack;
- dimensional stability in service;
- strong adhesion to metallic and nonmetallic surfaces;
- effective passivation of reinforcing steel;
- low permeability to fluids and chloride ions;
- low cost;
- beneficiation and/or valorization of industrial wastes; and
- low CO<sub>2</sub> emissions footprint.

Each of these benefits is certainly achievable through tailoring of a binder system, and a well-designed material with low water/binder ratio can probably achieve most of the above-listed characteristics. However, a single formulation is unlikely to be optimized in all these areas, so the material must be tailored to the desired application.

Given this high degree of commercial and academic interest in AAMs, it is timely to provide a review of the fundamental aspects of chemistry and materials science that control the formation of these alkali-activated binder systems. This review also provides insight into the pathways by which such systems may be further optimized, developed, and utilized. This review discusses primarily the materials science underpinning the chemistry, microstructure, and design of AAMs. For a detailed discussion on AAM performance in particular applications, the reader is referred to the recent *State-of-the-Art Report* of the RILEM Technical Committee 224-AAM (7).

## 2. ALKALINE-ACTIVATING SOLUTIONS

The most apparent difference between an alkali-activated binder and a traditional Portland cement is that the hardening of Portland cement is induced simply by mixing with water, whereas alkali activation requires the addition of an alkaline component in aqueous form. Thus, it is relevant to introduce the characteristics of the alkaline solutions used in this application. The solutions to be discussed are hydroxides and concentrated alkali metal silicates. There are applications in which alkali metal carbonates or sulfates are also useful in alkaline activation (7), but these fall beyond the scope of the current review.

### 2.1. Alkali Hydroxides

The hydroxide solution most commonly used as an alkali activator is sodium hydroxide; potassium hydroxide sees some use in specialized applications, whereas lithium, rubidium, and cesium hydroxides are of limited large-scale application (28). Alkali hydroxides are generally produced electrolytically from chloride salts, which introduces some energy usage and associated CO<sub>2</sub> emissions into the AAM production process, although the exact emissions accounting around this process depends on whether the chlorine that is also generated in this process is considered to be a valuable commodity or a by-product (29).

If an alkali hydroxide activator is used in an AAM mix design, its concentration will often exceed 5 molal, particularly when low-calcium aluminosilicates (metakaolin or low-calcium fly ash) are used as solid precursors (7, 28). This high concentration can lead to significant occupational health

**Efflorescence:** the development of salt deposits on the surface of a porous building material; often caused by the reaction of cations leached from the pore solution with atmospheric CO<sub>2</sub>

**Gel:** in a cementitious binder, the hydrous disordered silicate material that fills space and provides strength; often composed of nanoparticulate units with partially ordered local structure

and safety considerations in a large production facility, as such solutions are classified as corrosive under workplace legislation in force in almost every country in the world (8). Hydroxide-activated fly ash materials also generally require thermal curing [60°C or higher, depending on the reactivity of the fly ash (30)], which is acceptable in precast concrete production but causes difficulties for on-site operations. Hydroxide-activated binders, whether based on fly ash or on BFS, also tend to show higher permeability than their silicate-activated counterparts (31) and a tendency toward efflorescence because the extent of reaction reached by the binder before hardening is often low, which leads to an open microstructure with a mobile, alkali-rich pore solution. Efflorescence and other visible effects of alkali mobility are obviously undesirable but can be overcome to some extent by appropriate control of curing conditions or addition of secondary aluminum sources to ensure that a sufficient extent of reaction is reached before the material is placed into service (32).

Despite the shortcomings listed above, there are circumstances in which a hydroxide activator can provide benefits in certain aspects of technical performance. One such benefit is the outstanding dimensional stability of a hydroxide-activated fly ash geopolymer to temperatures of ~1,000°C (33), as shown in **Figure 3**. This stability is attributed to the very high degree of connectivity of the silicate gels in these binders, in which the use of a silicate activator leads to a small but nonzero content of silanol groups (partially depolymerized Si sites), which lose water upon heating and cause the characteristic expansion of these underconnected gels (33). Hydroxide-activated mixes can also show more favorable workability than silicate-activated binders because the viscosity of concentrated alkali hydroxide solutions is much lower than that of alkali silicate solutions of comparable concentration.

## 2.2. Alkali Silicates

As for the alkali hydroxide solutions discussed above, the silicate solutions of greatest interest in alkaline activation are those containing sodium or potassium as the alkali cation (28). Alkali

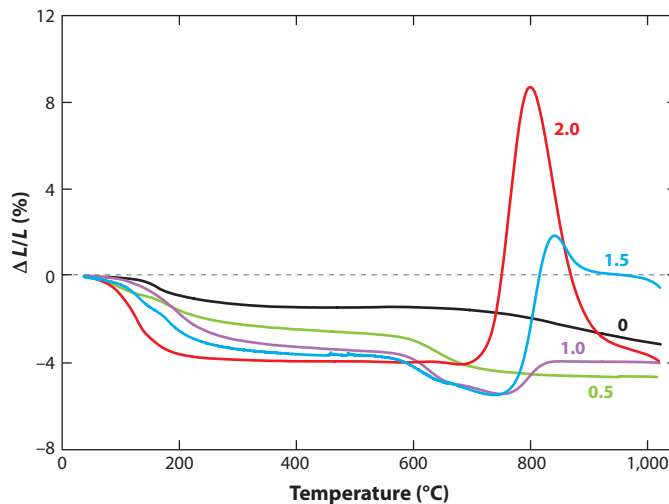


**Figure 3**

Dilatometric data showing the dimensional stability of alkali-activated fly ash as a function of temperature. All samples are formulated with a constant alkali/ash ratio, with differences in the SiO<sub>2</sub>/Na<sub>2</sub>O molar ratio of the activator as marked. Modulus 0 corresponds to a specimen activated by NaOH; all others are sodium silicate activated. Specimens were cured for 3 days at 40°C and then at room temperature for a further 4–7 days prior to testing. Data from Reference 33.

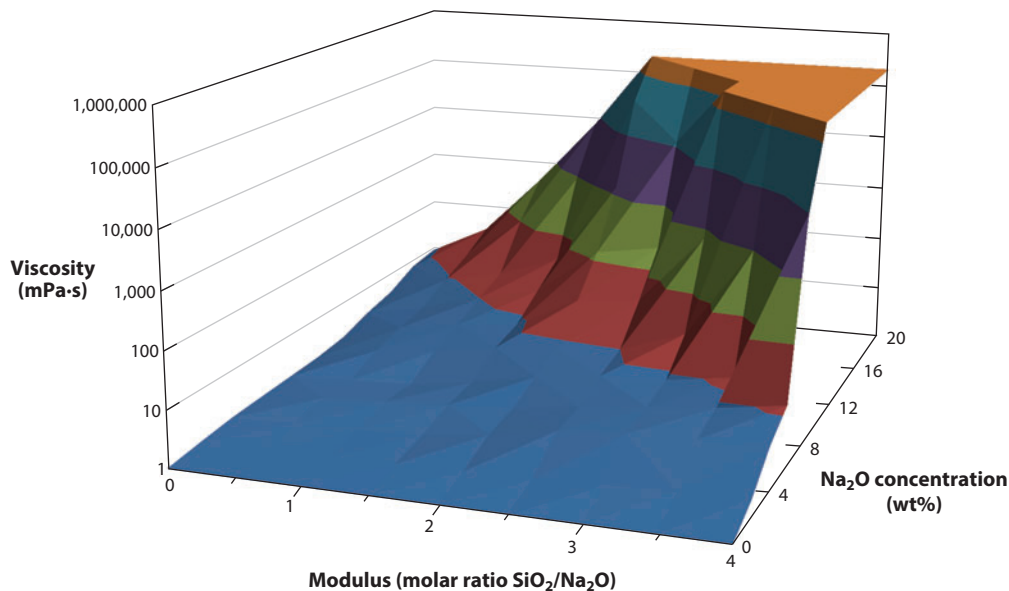


**Figure 4**

Viscosity of sodium silicate solutions as a function of modulus and  $\text{Na}_2\text{O}$  concentration, showing the dramatic increase in viscosity beyond a threshold modulus and  $\text{Na}_2\text{O}$  concentration, which causes the loss of workability of geopolymer pastes produced with high activator concentration and modulus. Data from Reference 37.

silicates are generally produced from carbonate salts and silica via melting to form a glass. This glass is then dissolved in warm water to form a viscous, sticky solution, also known as water glass.

The chemistry of silicon is probably richer than that of any other element except carbon, but this richness still remains relatively unexplored and poorly understood. In concentrated alkaline solutions, silica polymerizes into a complex array of oligomeric species containing between 2 and 15 monomeric units each, in equilibrium with a population of isolated monomers (34, 35). In the context of alkali activation, the relative reactivities of these species are a function of their size; monomers are the most reactive and thus the most important in the context of geopolymerization (36). Monomeric silica  $[\text{Si}(\text{OH})_4]$  is a polyprotic weak acid, buffering the pH in the range of 11–13.5 for the solution compositions of interest in alkaline activation, but provides a much higher level of available alkalinity than do hydroxide solutions of comparable pH due to this buffering effect. This lower pH is a major benefit in industrial handling, in which some silicate-activated binder systems can be classified as irritants rather than as corrosive and so are much more suitable in a large-scale processing context (8).

The major drawback associated with the use of alkali silicate solutions in alkaline activation is related to the often very high viscosity of these solutions. **Figure 4** presents the viscosities of sodium silicate solutions as a function of composition at room temperature. Viscosities are plotted on a logarithmic scale and increase dramatically at higher silica content.

Potassium silicate solutions show a much lower viscosity than do sodium silicates of comparable composition on a molar basis, by a factor of as much as  $10^4$  in the high concentration/high modulus range of interest here (37). This difference may be conceptualized by considering the hydration properties of the cations present in each of the solutions.  $\text{Na}^+$  is a moderately strongly hydrated cation that tends to take on a coordination number of approximately 6 in its first hydration shell.

---

**Modulus:** the molar ratio  $\text{SiO}_2/\text{M}_2\text{O}$  of an alkali silicate, where M is an alkali metal

---

However, in a sodium silicate solution of modulus 1.0 at 5 molal (19.2 wt%)  $\text{Na}_2\text{O}$ , which is fairly typical for production of a geopolymer from fly ash or metakaolin, there are approximately 5.5 molecules of water present per  $\text{Na}^+$ . This quantity of water is not sufficient to fully hydrate all the  $\text{Na}^+$  cations present, and although some ion pairing with silicate anions will certainly take place, it is reasonable to suggest that the number of freely mobile water molecules in such a solution will approach zero. Thus, the standard discussion of aqueous solution chemistry may begin to break down in such cases because defining water as a solvent when its motion is so restricted is no longer possible; the so-called solution may be closer to an ionic liquid on a nanostructural level, which is in part responsible for the very high viscosities observed when large quantities of silica are also present. Conversely,  $\text{K}^+$ , a relatively weakly hydrated cation, does not restrict the motion of water to the same extent as  $\text{Na}^+$ , so a concentrated potassium silicate solution is able to flow with much less restriction.

This behavior also holds for the fresh alkali-activated binder pastes; potassium silicate-activated aluminosilicate binders show much more favorable rheological properties than do their sodium silicate-activated counterparts. This difference in rheology is controlled from a fundamental chemical level according to the availability of water in the binder systems. The silicon dissolving from the solid precursor can also cause a dramatic increase in viscosity in the aqueous phase (**Figure 4**), although this increase may be dominated by the influence of calcium and/or aluminum in inducing gel formation, stiffening, and setting, as discussed in the following sections.

### 3. STRUCTURE AND CHEMISTRY OF HIGH-CALCIUM ALKALI-ACTIVATED BINDERS

#### 3.1. Gel Chemistry of High-Calcium Alkali-Activated Systems

In discussions of the chemistry of alkali-activated binders, it is essential to first classify these systems according to the types of gel that dominates the structure. This distinction is drawn mainly on the basis of the calcium content in the system, as shown in **Figure 5**, in which the primary reaction product is either an alkali aluminosilicate-type gel or a calcium (alumino)silicate hydrate (C-A-S-H<sup>1</sup>)-type gel. The first of these gel types (the right-hand pathway in **Figure 5**), which is poor in calcium, is often represented as N-A-S-(H) but can also show substitution of potassium (up to 100% replacement of sodium) or substitution of calcium for sodium, so a more complete description may be N,K-(C)-A-S-(H). (Substitution limits for calcium are not yet well known and are the subject of ongoing research.) In the right-hand pathway in **Figure 5**, the H is shown in parentheses to indicate that the water is not a major structural component of this gel, as it is in C-A-S-H-type gels (38). The C-A-S-H-type gels (the left-hand pathway in **Figure 5**) almost always coexist with secondary products of the layered double-hydroxide group, which are explored in more detail in Section 3.2.

For the purposes of discussing AAMs, a high-calcium binder system is defined as having a  $\text{Ca}/(\text{Si} + \text{Al})$  ratio of approximately 1; such materials are most commonly produced by the

---

<sup>1</sup>Cement chemists abbreviate chemical formulae in oxide units. Abbreviations used in this review are: S to represent  $\text{SiO}_2$ , A for  $\text{Al}_2\text{O}_3$ , C for  $\text{CaO}$ , N for  $\text{Na}_2\text{O}$ , K for  $\text{K}_2\text{O}$ , and H for  $\text{H}_2\text{O}$ . Minor or optional components, potentially absent from the gel structure, are shown in parentheses, and the hyphens between symbols indicate nonstoichiometric compounds. So, for example, the hyphenated formula C-(A)-S-H represents a nonstoichiometric calcium silicate hydrate with possible partial alumina substitution, whereas CH (with no hyphen) is a stoichiometrically correct representation of portlandite [ $\text{Ca}(\text{OH})_2$ ]. The C-A-S-H-type gels discussed in this review are shown without parentheses to highlight the important role played by aluminum in their structure, as distinct from the gels formed by Portland cement hydration, in which aluminum substitution is generally a minor effect.

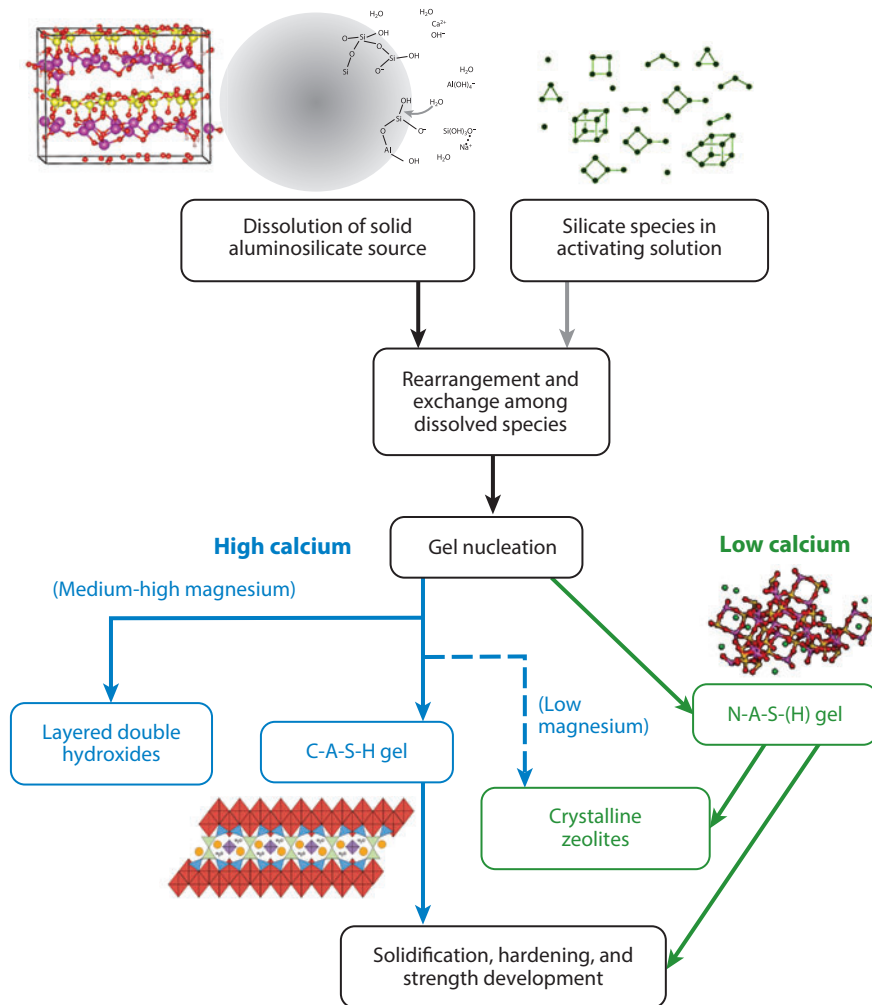


**Figure 5**

Process and reaction products of alkaline activation of a solid aluminosilicate precursor. High-calcium systems react according to the left-hand (*blue*) pathway, with the nature of secondary products determined by Mg content, whereas low-calcium systems react according to the right-hand (*green*) pathway. For each type of precursor, hydroxide activation tends to increase the ratio of crystalline to disordered products compared with silicate activation.

interaction of BFS with alkaline solutions. BFS will very slowly react with water to form a hardened binder (39), and so the key role of the alkaline activator is to accelerate this reaction, enabling the material to harden and develop strength within hours to days. This process yields the early-age engineering properties (strength and stiffness) that are essential in construction materials.

A number of reviews have discussed in detail the chemistry and basic engineering aspects of alkali-activated BFS-based binders (e.g., 7, 10, 40–42). These are the most mature commercially applied AAM materials systems worldwide (9), and the presence of calcium is now recognized to enhance many aspects of AAM concrete durability due to its role in reducing permeability (43), which is essential in extending concrete service life.

**Dreierketten:** the repeating unit of three silicate tetrahedra—two paired sites and one bridging site—that is the dominant structural motif in a tobermorite-like silicate phase or gel

The effect of the activator pH on the activation of BFS is both important and sometimes seemingly counterintuitive. Calcium solubility is reduced at higher pH as supersaturation is reached with respect to portlandite  $[\text{Ca}(\text{OH})_2]$ , and thus hardened hydroxide-activated binders (initial activator pH > 14) often show a much lower overall extent of reaction and lower mechanical strength than do silicate-activated systems (initial activator pH  $\sim 11$ – $13.5$ ) (44, 45). The silicate species supplied by the activator react with the calcium and aluminum (and additional silicon) supplied by the dissolving BFS to form solid binder products. This gel formation process removes calcium from the solution phase and so further drives BFS dissolution and enhances the overall extent of reaction.

### 3.2. Alkali Activation of Blast Furnace Slag: C-A-S-H and Secondary Products

In studies assessing the reaction products formed by alkaline activation of BFS, the consensus is that the main reaction product is an aluminum-substituted C-A-S-H-type gel (40, 46–50) having a disordered tobermorite-like structure (**Figure 6**). Independent of the activator used, the C-A-S-H-type gel formed through the activation of BFS has a lower calcium content than a hydrated Portland cement system, whose Ca/Si ratio is usually between 1.5 and 2.0. The C-A-S-H product formed in NaOH-activated BFS generally has a higher Ca/(Si + Al) ratio and a more ordered nanostructure [observable through somewhat sharper X-ray diffraction (XRD) reflections] than in silicate-activated binders (46, 51), although the precise chemical composition depends on the chemistry of the BFS; this topic is further explored below. The exact nature and degree of the structural disorder in calcium silicate hydrate gels have been discussed recently, including arguments that the apparently disordered nature of the C-S-H resulting from hydration of tricalcium silicate ( $3\text{CaO} \cdot \text{SiO}_2$ ) is actually largely due to the very small ( $<4$ -nm) fundamental crystallite size, rather than being a chemical structural effect (52). In the case of gels in which calcium and silicon are substituted partially by alkalis and aluminum, respectively, as in **Figure 6**, a significant degree of nanostructural disorder is also highly likely, as determined by Puertas et al. (50) using molecular dynamics. This nanostructural disorder is also consistent with the model calculations of Myers et al. (48), which required a mixture of cross-linked and non-cross-linked tobermorite phases to accurately capture the chemistry of these materials on a structural level.

As in Portland cement systems, the C-A-S-H gel includes layers of tetrahedrally coordinated silicate chains with a dreierketten structure, each chain containing  $(3n - 1)$  tetrahedra for an integer value of  $n$ , as depicted in **Figure 6**. The interlayer region contains  $\text{Ca}^{2+}$  cations, alkalis, and the water of hydration that is chemically incorporated into the gel structure. Some alkali cations also balance the net negative charge generated when  $\text{Al}^{3+}$  replaces  $\text{Si}^{4+}$  in the tetrahedral chain sites.

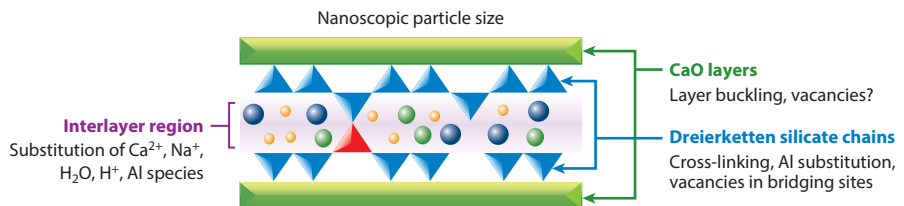


**Figure 6**

Tobermorite-like C-A-S-H gel structure. The triangles denote tetrahedral Si sites (the *red triangle* denotes Al substitution into one bridging site), the green rectangles denote CaO layers, and the circles denote various interlayer species. Mechanisms by which crystallographic disorder can be introduced into the gel structure are listed in italics.

Because of the chemical limitations imposed by the constraints of the tobermorite-like structure, the extent of uptake of aluminum and magnesium into the primary binding phase is limited. The incorporation of tetrahedral aluminum into C-A-S-H chains takes place predominantly in the bridging tetrahedral sites shown in **Figure 6** (48, 53–56), and some aluminum can also be located in interlayer sites. This strong preference for substitution on specific sites places a structural limitation on the total Al/Si ratio, which is constrained to a value of less than 0.20, depending on the degree of cross-linking of the gel (lower in cross-linked than in non-cross-linked gels) (48). Magnesium incorporation into C-A-S-H-type structures is also very limited because the ionic radius of  $\text{Mg}^{2+}$  is not a good match for the  $\text{Ca}^{2+}$  sites in the tobermorite-type structure.

Thus, the formation of C-A-S-H gels by alkaline activation of slags containing significant quantities of aluminum and/or magnesium (which is almost always the case) results in the formation of a C-A-S-H gel accompanied by secondary aluminum- and/or magnesium-rich reaction products, as depicted in **Figure 5**. The commonly observed secondary products are AFm-group layered hydrous calcium aluminates, hydrotalcite-like (Mg,Al)-layered double hydroxides, and/or zeolites such as gismondine and garronite when the availability of MgO is low (7, 57–59), as depicted in **Figure 5**. AFm phases are not always identifiable by XRD, but studies of elemental composition correlation charts obtained by elemental analysis in an electron microscope suggest that AFm-like layers are intimately intermixed into the C-S-H structure on a nanometer length scale (57, 60, 61).

Alkalis play a crucial role in determining AAM gel properties and structure (20) because of the high concentration of alkalis in an AAM binder system, which can be as high as 5 mol/kg binder in some cases (but is more often on the order of 1–2 mol/kg binder). The effect of alkali oxides (particularly  $\text{Na}_2\text{O}$ ) on the composition and microstructure of calcium silicate hydrate gels has been widely studied (62–66). However, there is still no real consensus on the most important mechanism determining the interactions between these species in the pore solution and the solid binder components at very high pH, particularly the influence of aluminum on the uptake of alkalis by the binding gel. Conceptually, this uptake likely depends on both  $\text{Ca}/(\text{Al} + \text{Si})$  and  $\text{Al}/\text{Si}$  ratios within the gel, but further systematic work is required in the compositional region of interest in alkali-activated systems to unravel both kinetic and equilibrium effects in these systems.

The incorporation of alkalis into the C-A-S-H-type gel will commence from the very early stages of reaction in an alkali silicate-activated BFS binder, that is, when the effective Ca/Si ratio in the fluid phase is very low due to the low extent of dissolution of the solid precursor and when the Na/Ca ratio is therefore high. The uptake of alkalis in those initially formed gels is thus expected to be much higher than in the C-S-H gels formed in conventional Portland cement systems. However, Hong & Glasser (63) also observed that alkali binding decreases with increasing Ca/Si ratio in C-S-H gels, which may indicate that the ongoing provision of calcium from slowly reacting BFS particles can lead to the rerelease of alkalis from C-A-S-H phases that were initially alkali rich. This process may have important implications in terms of the long-term phase chemistry of the binders formed; the tobermorite-like gel structure is stable for many hundreds of years in the presence of aluminum, as evidenced by analysis of ancient Roman concretes (67), but the influence of higher concentrations of alkalis on this stability remains under analysis. Microstructural analysis of alkali-activated slag concretes aged for 8–30 years (68–70) has shown high stability, ongoing increases in mechanical strength, and no evidence of any type of deleterious chemical reaction processes involving C-A-S-H gel instability. However, further work in this area is warranted, particularly with regard to the long-term evolution of mechanical properties such as creep under applied load (7).

---

**AFm (aluminoferrite-mono) phase:**  
a family of layered hydrated calcium aluminate phases similar to hydrocalumite, with anion substitution

---

---

$Q^n(mAl)$ : notation to describe the coordination of a tetrahedral silicon atom, bonded via oxygen to  $n$  other tetrahedral atoms,  $m$  of which are aluminum;  $0 \leq m \leq n \leq 4$

---

### 3.3. The Influence of Slag Chemistry

The chemical composition of BFS is often described within the quaternary system CaO-MgO- $Al_2O_3$ - $SiO_2$ . Additional components, including manganese, sulfur, and titanium, are also present in most slags, depending on the chemical composition of the iron ore used. Rapid cooling of molten BFS leads to a glassy structure, which is necessary to yield a reactive material, as slow-cooled slags tend to crystallize and are poorly reactive. In general, glassy BFS with CaO/ $SiO_2$  ratios near 1 and containing some (15–30% total)  $Al_2O_3$  and MgO is amenable to alkali activation (71). Sulfur is usually present in reduced form, which leads to a negative redox potential in the pore solution of slag-based binders. This negative redox potential can be very valuable in some specialized applications involving immobilization of hazardous or radioactive transition metals (72). The compositional differences among BFS produced in different parts of the world have historically led to some limitations in developing a fully generic understanding of high-calcium AAM binder structure because (a) the secondary phase assemblages formed from different types of slags have not always been well described in the literature and (b) the chemistry of the C-A-S-H-type gel has only recently been described in detail, as discussed in Section 3.1.

The presence of higher levels of MgO in the BFS used to make an AAM can enhance the strength of the binder (73, 74), which is linked to the formation of hydrotalcite-type products (73). Magnesium also appears to increase resistance to carbonation (75). This increased resistance is correlated with the presence of hydrotalcite-group phases, which are formed with MgO/ $Al_2O_3$  ratios ranging from 4 to 6 [i.e., from quintinite to hydrotalcite in the preferred mineralogical nomenclature (76)], depending on the relative magnesium and aluminum contents of the slag (47, 49, 60, 75). These reports indicate that the formation of hydrotalcite—which is not itself believed to be a particularly strength-giving binder phase—leads to an improvement in strength that may be related to a reduced level of aluminum incorporation into the C-A-S-H gel. Increased  $Al_2O_3$  content in the BFS reduces the extent of reaction at early times of curing and consequently decreases the compressive strength of activated BFS binders (77), although the specific effect of aluminum incorporation on the mechanical properties of C-A-S-H-type gels is not yet clear. Recent direct measurements of the bulk modulus of pure and aluminum-substituted C-S-H using a diamond anvil cell and synchrotron radiation did not show any significant differences as a function of aluminum content (78). Thus, further investigation is required to determine in detail the parameters that control the correlation between slag chemistry and the mechanical performance of high-calcium AAMs.

## 4. STRUCTURE AND CHEMISTRY OF LOW-CALCIUM ALKALI-ACTIVATED BINDERS

### 4.1. Gel Chemistry of Low-Calcium Binders

The fundamental binder in low-calcium alkali-activated systems is a structurally disordered, highly cross-linked aluminosilicate gel (79): the N-A-S-(H) product described briefly above and depicted in the right-hand pathway in **Figure 5**. Both silicon and aluminum are present in tetrahedral coordination; silicon is predominantly in  $Q^4(mAl)$ -type environments in which the distribution of  $m$  values depends on the Si/Al ratio of the gel (80). The negative charge associated with substitution of silicon by tetrahedral aluminum is balanced by the association of alkali cations with the gel framework. There are similarities between this gel structure and the structure of zeolites (24, 81). Provis and colleagues (79) proposed that the chemical similarities between the process of hydrothermal synthesis of aluminosilicate zeolites and the reaction of low-calcium AAMs mean that the disordered gel is likely fundamentally zeolite like in a chemical sense but disordered on any

length scale beyond several angstroms. X-ray and neutron pair distribution function analysis later confirmed this possibility directly (82, 83). Such analysis showed that, on length scales of up to 5–8 Å, the local structures of metakaolin-derived aluminosilicate binders are very similar to the local structures of crystalline zeolitic (particularly analcime-group) structures with corresponding Si/Al ratios.

This information then provides a useful structural model by which the nanostructurally determined properties of these materials, such as thermochemistry (84) and ion exchange (85), can be understood and tailored (86). This approach is approximately analogous to the use of tobermorite as a model structure for the understanding of the C-A-S-H gels discussed in Section 3. Most importantly, this approach enables the design of material formulations that are suitable for desired applications. The key applications for low-calcium AAM technology fall into two distinct fields: (a) use as a cement-like binder (for example, in production of tiles, pavers, precast concrete, or ready-mix concrete, in which mechanical and physicochemical durability properties are essential for success) or (b) use as a low-cost alternative to fired (dense or porous) ceramics, such as mullite or alumina, in which optimized thermal characteristics may become important (7, 27).

## 4.2. Alkali Activation of Metakaolin

Metakaolin is the disordered, partially dehydroxylated product of the thermal treatment of kaolinitic clays at temperatures of ~500–800°C, which are below the temperature at which the material recrystallizes to mullite,  $3\text{Al}_2\text{O}_3 \cdot 2\text{SiO}_2$  (87). Kaolin can be mined directly as a pure mineral or sourced in less-pure form from mine tailings or paper industry wastes. These different sources induce differences in particle size, purity, and crystallinity—properties that influence reactivity (88). But the fact that alkaline activation offers a pathway to valorization of impure or low-grade clays provides some scope for cost reduction compared with the cost of commercial metakaolins, which are generally derived from high-purity clay deposits.

Although metakaolin is derived from a crystalline, layered clay mineral structure, it does not show long-range crystalline order but rather has a disrupted residual layered structure (89), which plays a large role in making it suitable as a geopolymer precursor. The reactivity of metakaolin in an alkaline environment is provided by the crystallographically strained aluminum sites within the formerly octahedrally coordinated layer of kaolinite (90). Kaolinite loses its ordering and bound hydroxyl groups upon heating, resulting in the formation of energetic Al-O-Al bonds and rendering the aluminum very readily available for reaction. The dissolution of the aluminum layers from the layered particles also leaves the silicon sites accessible to the alkaline solution, which makes metakaolin a highly reactive precursor under alkali activation conditions. **Figure 7** illustrates the pathways by which kaolinite is converted, via metakaolin as an intermediate, into either mullite (by further thermal processing) or a geopolymer (by alkaline activation). The calcination of kaolinite at temperatures between 500 and 750°C induces a stepwise process of dehydroxylation and structural disordering by buckling of the layered clay structure (91), which is responsible for the reactivity of metakaolin under alkaline conditions, whereas either undercalcined or overcalcined products would be unreactive in alkali activation.

The characterization of alkaline-activated, low-calcium aluminosilicate binders by nuclear magnetic resonance has shown the predominance of  $\text{Q}^4(n\text{Al})$  sites, with  $n$  distributed between 1 and 4 but usually at the higher end of this range for hydroxide-activated systems (80, 92). The concentration of bound hydroxyl groups (i.e.,  $\text{Q}^3$  silicate sites) is low in well-cured binders with hydroxide or low- or moderate-modulus silicate activators (93). A higher silicate concentration is required before these sites are notable in well-cured materials, although they are certainly present at early age at all Si/Al ratios. Thus, the water in a fully cured, metakaolin-derived binder is mainly

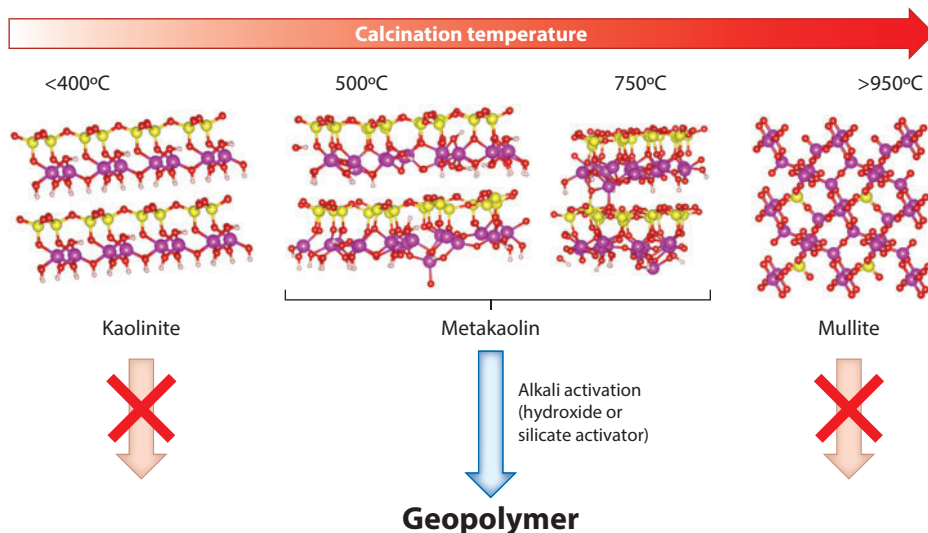


**Figure 7**

Pathways for the conversion of kaolinite to economically valuable products: calcination at moderate temperatures (500–750°C) followed by alkaline activation to form a geopolymer, or calcination beyond 950°C to form mullite. Metakaolin structural sketches are based on data in Reference 91.

either (a) physisorbed as molecular  $\text{H}_2\text{O}$  on the gel surface or (b) free and mobile within open pores, as shown by thermal analysis (94), nuclear magnetic resonance (NMR) spectroscopy (93), and gas sorption coupled with positron annihilation lifetime spectroscopy (95).

The crystallites formed in NaOH-activated metakaolins (with overall Si/Al ratios close to 1.0) are predominantly sodalite-type feldspathoids with either  $\text{OH}^-$  or  $\text{H}_2\text{O}$  as the intracage species. Some zeolitic phases, particularly NaA and/or NaX [classified as the LTA and FAU framework types (96)], are also observed either as transient phases that convert to hydrosodalite at more extended curing durations or as final reaction products (Figure 5) (97, 98).

The binder gel nanostructure formed by silicate activation of metakaolin is rather similar to that of the hydroxide-activated gels, although generally favoring lower values of  $n$  in the distribution of  $\text{Q}^4(n\text{Al})$  sites (80). Because the increased pH of lower-silicon systems accelerates crystallization of the gel, and because most of the favored zeolite products in these binders have Si/Al ratios of between 1 and 2, gels with higher Si/Al ratios are more resistant to crystallization. The microstructure of a silicate-activated metakaolin binder system tends to be more homogeneous than that of a hydroxide-activated binder on a length scale of micrometers or more (99, 100), as the lower-silica gels tend to form into discrete particulate units rather than generating a continuous gel network. The presence of silicate in the activator also yields a much higher compressive strength and elastic modulus and a lower porosity in silicate-activated binder systems (99, 101, 102) when the activator modulus is between 1 and 2. Beyond this optimum, which depends on the nature and chemistry of the aluminosilicate precursor, the extent of reaction decreases as the pH of the fresh geopolymer paste is reduced by the high  $\text{SiO}_2$  content, and the increased viscosity (Figure 4) hinders diffusional transport of species to and from the particle surfaces. A binder gel with an Na/Al ratio of close to 1 also seems to give the best combination of strength and resistance to efflorescence, consistent with the role of aluminum in balancing the gel framework charge (79, 98).

Metakaolin has also been identified as a key component of several useful precursor blends. For example, combinations with fly ashes and various slags supply additional aluminum to the reaction

process (103), thus tailoring reaction rates and thermal properties (104, 105). This blending pathway may also address the workability issues discussed above and provides a good deal of scope for future developments in the area.

Kaolinite is not the only clay mineral that has been successfully utilized in alkaline activation. A research program in Portugal used thermally treated muscovite-rich waste obtained from a tungsten mine in the production of binders, concretes, and specialized systems for concrete repair applications (106), yielding high-strength binders from a relatively wide range of formulations. Illite-smectite clays have also proven to be amenable to alkali activation; the high Si/Al ratio of these clays favors the use of a low-silica activating solution to give optimal binder performance (107). Pyrophyllite clays have not been able to be thermally treated to provide a suitable source material for alkaline activation (108), possibly because, unlike the case of kaolinite, the dehydroxylation product of pyrophyllite has a relatively well ordered structure (109). Mechanochemical processing has generated the necessary reactivity for both pyrophyllite (108) and halloysite (110) to produce good strength development rates under alkaline activation.

### 4.3. Alkali Activation of Fly Ash

Fly ash is a by-product of coal-fired electricity generation. It is the incombustible mineral associated with the coal, comprising predominantly aluminosilicate remnants of minerals associated with the coal deposit. Fly ash passes through the boiler furnace and is collected in the chimneys by electrostatic precipitators. Fly ash particles are often vitreous, close to spherical, and sufficiently reactive to be of value in alkali activation.

Fly ash is almost always activated by alkali hydroxide or silicate solutions. The gel binder structures formed by alkali activation of low-calcium fly ash are similar to those of the metakaolin-based geopolymer gels (111), with highly cross-linked, tetrahedral N-A-S-(H)-type gel structures, as discussed in Section 4.1 (97). The gel binder structure is closely related to that of the precursor gels observed as intermediates during the hydrothermal synthesis of zeolites from the same aluminosilicate solids (79). Analyzing the gel connectivity of fly ash-based AAMs using NMR spectroscopy is difficult because of the nonzero levels of iron within almost all fly ashes (57, 112, 113). However, the results show that the fly ash-derived binder gel is predominantly  $Q^4$  in nature, with a distribution of  $Q^4(1Al)$  site environments, depending on the Si/Al ratio of the reactive component of the fly ash and on the amount of silicon supplied by the activator.

Crystalline zeolites and related phases also develop in these materials over a more extended curing time (**Figure 5**), with higher temperatures and higher water contents favoring the development of more crystallinity. Thermal or steam curing is usually applied to alkali hydroxide-activated fly ash binders, as strength development is slow at room temperature in these systems (30, 92). Thermally cured NaOH-activated fly ash binders tend to form chabazite-Na (also known as herschelite), faujasite, sodalite-group, and cancrinite-group secondary phases identifiable by XRD within the disordered bulk gel binder (101, 114, 115).

Despite the highly heterogeneous and structurally disordered nature of fly ash-containing alkali-activated binders (**Figure 8**), the understanding of the binder structure and chemistry of fly ash-based AAMs has recently been advanced by the application of Fourier transform infrared (FTIR) spectroscopy in both bulk and surface-sensitive analysis modes (115–120). The study of simplified model binder systems (116) has provided useful insight into the structure and formation of the N-A-S-(H) gel products as they grow on the surfaces of fly ash particles.

Using FTIR to study the reaction mechanism of fly ash geopolymer formation, Fernández-Jiménez & Palomo (117) proposed two stages of gel evolution: gel 1, which was relatively enriched in aluminum, and gel 2, which showed greater incorporation of silicon. However, if one considers

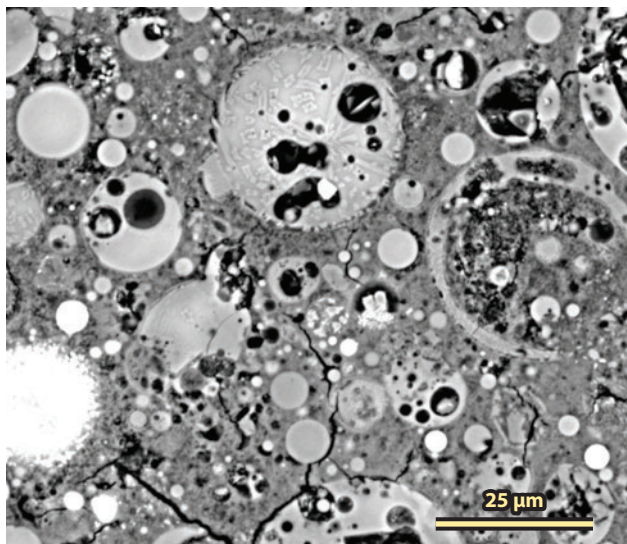


**Figure 8**

Scanning electron microscopy image of a polished section of a fly ash geopolymer that is activated by  $\text{Na}_2\text{SiO}_3$  solution. The interparticle and intraparticle heterogeneity of the fly ash precursor is evident, and the binder gel adheres closely to the surfaces of residual partially reacted particles. Some of the initially hollow particles have become filled with binder gel during the reaction process, whereas others still contain voids. Image courtesy of I. Ismail, University of Melbourne/University of Malaysia Sarawak.

the fact that FTIR measures bond vibrations rather than atomic nuclei, the distinction between aluminum-rich gels and silicon-rich gels should be revisited. The gel 1 stage involves a high degree of formation of Si-O-Al bonds relative to the overall Si/Al ratio of the binder system because cross-linking involving aluminum atoms is preferred over the formation of Si-O-Si bonds (118); i.e., the presence of nonbridging oxygen sites on silicon atoms is preferred over their presence on aluminum atoms. The result is a gel that may or may not be chemically enriched in aluminum but that does have a relatively high concentration of Si-O-Al bonds as observed by FTIR. Later gel structural evolution leads to further cross-linking via condensation reactions between Si-OH groups, resulting in an apparent increase in the Si/Al ratio of the gel as measured by FTIR, because Si is now participating to a fuller extent in the  $\text{Q}^4$ -dominated gel. This preference for Si-O-Al bonding also explains why the gel formed in a system with a solid aluminosilicate precursor and a silicate activator—with an initially high Si/Al ratio in the solution phase—can still appear relatively aluminum rich at early age (36), when bulk chemical considerations would indicate that the Si/Al ratio should decrease monotonically as aluminum is progressively released from the solid precursor particles.

The identification of two sequential stages in the gel formation process, approximately consistent with the shift from a  $\text{Q}^3$ -type gel to a  $\text{Q}^4$ -type gel, has also been supported by mathematical modeling of the reaction process (36) and by the combination of in situ attenuated total reflectance FTIR with ex situ bulk and spatially resolved FTIR analysis, to demonstrate the chemical mechanisms involved in the evolution from the initial to final gel structures (115, 119, 120). By using the analogies between the gels formed in fly ash-based and metakaolin-based binders, in situ energy-dispersive synchrotron XRD analysis of reacting pastes (121), rheological studies (122), and neutron pair distribution function analysis (123) of metakaolin-based samples have also provided nanostructural information regarding the nature of the gel 1/gel 2 transition in

N-A-S-(H)-based binders, which appears to take place in a similar manner in these low-calcium systems regardless of the nature of the precursor.

#### 4.4. The Influence of Fly Ash Chemistry

Fly ashes sourced from different electricity-generating stations worldwide can differ very widely in bulk major element (Si/Al/Fe/Ca) composition, glass phase fraction, unburnt carbon content, alkali content, and particle size distribution, and there is also variation with time in the ash from a specific generating station as the blend of coal sources used in its furnaces is varied. Each of these parameters is vitally important to the reactivity and reaction process of a fly ash undergoing alkali activation and thus in determining the properties of the hardened binder resulting from this process.

The scientific literature contains lengthy discussions of the role of calcium supplied by fly ash in an alkaline activation process (102, 114, 124–127). Along with aluminum, calcium plays an essential role in determining the nature of the gels formed through alkaline activation. However, the factors controlling the glass reactivity that in turn determines the extent of gel formation possible in each binder system are much more complex. All alkali metal and alkali earth cations can act as network modifiers in aluminosilicate glasses, and thus their presence leads to a higher likelihood of forming a reactive glassy phase within the fly ash, rather than unreactive quartz or mullite. On the basis of this principle, Duxson & Provis (126) developed a simplified pseudoternary classification for fly ashes, as depicted in **Figure 9**, in which the chemistries are classified according to the strengths of the geopolymer binders formed (using data collated in Reference 126 for paste and mortar samples and reported in Reference 127 for concretes). The compositions of BFS from several

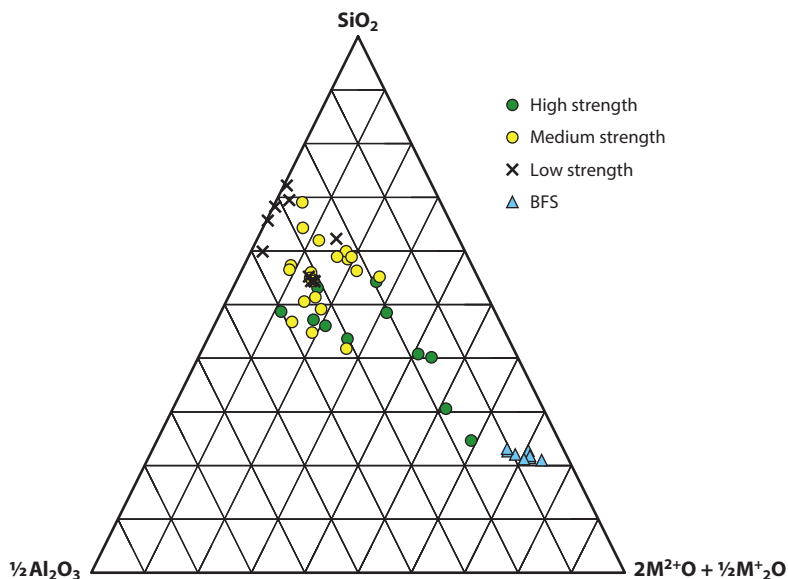


**Figure 9**

Representation of fly ash compositions in a pseudoternary system showing silica, alumina, and network-modifier [scaled alkali metal plus alkali earth (126)] oxide contents. The strength classification of geopolymer binders synthesized from each of the ashes is indicated in the legend. BFS denotes blast furnace slag. Data taken from the literature survey in Reference 126 for paste and mortar samples and from Reference 127 for concrete samples.

sources (taken from Reference 20) are also presented for comparison. The fly ash compositions are taken from bulk X-ray fluorescence data, not corrected for the presence of crystalline phases or of any other elements beyond those noted. Thus, this representation of the detailed chemistry of the system is necessarily oversimplified, particularly in the context of interparticle and intraparticle heterogeneity indicating that the bulk composition of the fly ash is very unlikely to be matched exactly by the glass chemistry of any single particle within the ash. Nonetheless, the simplicity of this approach to classification of fly ash chemistry provides interesting scope for use as a bulk prescreening method for ashes from different sources.

To this end, **Figure 9** shows that fly ashes containing low levels of aluminum and/or network modifiers will in general not result in satisfactory strength development when used as the sole precursors for alkali-activated binders; such ashes are generally poorly reactive (117, 128). Both aluminum and network modifiers are needed for high strength development, but even when these species are present, high strength development is also more likely when the unburnt carbon content is low and the particle size distribution is sufficiently broad to enable dense particle packing and to reduce water demand. Various authors reported that iron content has both positive and negative effects on reaction processes and strength; this area requires further attention from researchers. Possibly even more fundamentally, the ability to characterize (or even to define) the degree of reaction of fly ash is an area of ongoing research activity that is essential for a full understanding of alkali activation processes, as it is with fly ash-blended Portland cement binders (129).

## 5. BLENDED BINDER SYSTEMS AND GEL COEXISTENCE

Given that N-A-S-(H)-type gels offer the opportunity for production of binders with excellent chemical and thermal resistance (57, 104), whereas C-A-S-H-type gels provide chemical binding of water that reduces permeability (43), there is interest in synthesizing binders in which these two types of gel can coexist and each can contribute to the performance of the material (57, 130–132). The N-A-S-(H) gel may also offer some scope for anion-binding mechanisms that retard chloride ingress, thus increasing the service life of a reinforced concrete by prolonging the time taken to initiate corrosion of embedded steel (133). Gel coexistence requires a pH that is not high enough to cause the calcium to precipitate as portlandite (134, 135), which means that the use of moderate-pH activators such as alkali sulfates can be of value (136, 137). The combination of less reactive aluminosilicates with a smaller quantity of a more reactive calcium source such as BFS or Portland cement, with the addition of alkalis to accelerate the reaction process, also opens scope for the valorization of wastes or by-products that are insufficiently reactive to provide good strength development when either activated alone or blended with Portland cement in the absence of an additional alkali source.

The simplest model systems that can lead to this type of gel coexistence are those involving metakaolin, calcium hydroxide, and a moderate concentration of NaOH (135, 138), in which excessive alkalinity destabilizes the C-A-S-H-type gel and leads instead to the formation of N-A-S-(H) and portlandite. Similar gel coexistence trends have also been identified in BFS-metakaolin blended binders (139), and the distinct signatures of the two gel types are identifiable by the presence of two distinct mass loss peaks in thermogravimetric analysis (104). The dissolution of BFS is enhanced by the initial formation of C-A-S-H-type gels, which removes calcium from the solution phase and thus provides a driving force for continued reaction. The mechanical strength of these binders, and that of similar systems containing fly ash, appears to be enhanced when C-S-H and N-A-S-H gels coexist (134, 140, 141). The addition of a secondary source of calcium to a blended binder also tends to increase the  $\text{Na}^+$  concentration of the pore solution, consistent with the fact that this ion is less strongly bound in C-A-S-H-type gels than in N-A-S-(H)-type gels (125).

The combination of fly ash, BFS, and an alkaline activator has long been considered to be a promising route to the production of high-performance alkali-activated binders (142). Such systems can show excellent mechanical strength, reaching 100 MPa after 28 days of sealed curing at 23°C and continuing to increase in strength beyond this time when the precursors are appropriately selected and blended and the activator content and modulus are selected to match the precursor chemistry (143). However, BFS is much more expensive than fly ash in most parts of the world. Therefore, in many studies, it is added at a fairly small volume fraction into an otherwise fly ash-based binder system. For example, Li & Liu (144) found that 4% BFS enhanced the measured compressive strength of a 9:1 fly ash:metakaolin blend by more than 40%. The addition of a small amount of Portland cement into an alkali-activated binder system is also sometimes used to generate more rapid initial strength development.

The precise details of the gels formed in blended BFS–fly ash AAMs are strongly dependent on the blending ratio, composition, and relative reactivities of the solid precursors as well as on the selection of the activator. The reaction process continues well beyond the normal 28-day period of laboratory studies, with significant changes in gel and crystalline phase formation noted in these systems at up to 180 days (132). Hybrid C-N-A-S-H gels have been observed via elemental composition analysis by scanning electron microscopy–energy-dispersive X-ray spectroscopy (SEM-EDS) analysis (Figure 10). Such gels may result either from calcium substitution into N-A-S-(H)-type gels (with  $Q^+$  framework silicate structures) or from sodium sorption or substitution in chain silicate C-A-S-H-type gels (132, 145).

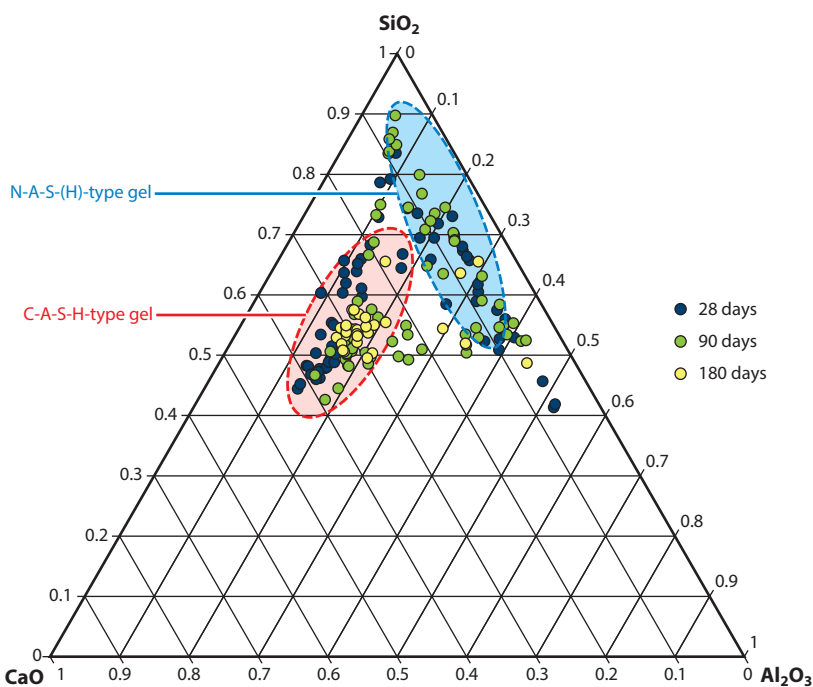


**Figure 10**

Elemental compositions measured for gel regions in a 1:1 fly ash:blast furnace slag binder activated by  $\text{Na}_2\text{SiO}_3$  solution, at ages of 28 days (blue), 90 days (green), and 180 days (yellow). The C-A-S-H-type gel (red dashed oval) appears to become more homogeneous with longer-term curing, whereas the N-A-S-(H)-type gel (blue dashed oval) remains more constant in composition. Data from Reference 132.

This discussion highlights the need for further detailed investigation of both synthetic and real gels within the  $\text{CaO-Na}_2\text{O-SiO}_2\text{-Al}_2\text{O}_3\text{-H}_2\text{O}$  system, at compositions and water/solid ratios relevant to the understanding of alkali-activated binders, so as to provide more detailed insight into the parameters that control gel formation kinetics and equilibrium composition, chemical and dimensional stability (including resistance to drying processes), and mechanical and transport properties. A more fundamental question underpinning many of these issues concerns the basic definition of different phases within a multiple-gel system, in which these materials may be intermixed so intimately that they are difficult to distinguish on a microstructural or bulk compositional level, necessitating the analytical application of high-resolution spectroscopic techniques. Moreover, there is also the question of what really constitutes a phase in a complex, disordered, hydrous material system. This type of discussion and analysis is essential for the prediction of the long-term stability and performance of alkali-activated binder systems. Such prediction is critical if these systems are to provide a viable alternative to Portland cement in large-scale construction applications and to contribute to the reduction of the environmental footprint of the global construction industry. Any material to be used in such essential applications must be well understood in terms of nanostructure and durability. Although the scientific and technical advances summarized in this review have provided a very good foundation for the initial deployment of this technology, much further analysis is required to fully describe AAMs and thus to optimize their performance in the service of humanity.

## 6. ENVIRONMENTAL ASSESSMENT

Discussions around the life-cycle analysis of alkali-activated binders have provided results that vary dramatically between mix designs and binder types (11, 12). The estimated  $\text{CO}_2$  savings (comparing AAMs with Portland cement) range from 9% to 97%, depending on the choice of alkali-activated binder mix design, the curing conditions specified, the nature of the Portland cement system selected as the reference, and the geographical parameters surrounding materials supply and transport. The details of these calculations are highly dependent on the location, mix design, and application selected for the material (11), so it is impossible to provide a single number that accurately represents the achievable emissions savings for AAMs compared with Portland cement concrete in a generic sense. The value of location-specific and application-specific case studies of environmental footprinting is therefore evident; only by comparing a particular alkali-activated mix design directly with a Portland cement-based material that it will replace directly in a specified application can a meaningful comparison be made. Emissions in noncarbon categories are also an important issue that requires further study (12), as is the need to improve and update the databases that underpin all such life-cycle calculations.

An important issue influencing the environmental assessment of alkali activation technology relates to the supply of raw materials, particularly the activator. As discussed in Section 1, some environmental impact is incurred through the production of the activators, particularly sodium silicate, which is most commonly produced from sodium carbonate and silica in a high-temperature process involving a glass intermediate. This high-temperature processing does bring associated energy consumption and  $\text{CO}_2$  emissions (146) that must be attributed to the silicate activator in any environmental assessment of an AAM. However, because the activator usually accounts for <10% by mass of an AAM binder, the  $\text{CO}_2$  emissions per tonne of binder are still much lower than the process  $\text{CO}_2$  emissions associated with Portland cement production according to the process shown in **Figure 1** (5, 11, 12). There are also significant differences in emissions depending on the source of the alkali carbonates used and the corresponding chemical or mining route employed. These differences can result in as much as a tenfold difference in emissions in

alkali-activated binders formulated in different ways, which can introduce some major geographical specificity into AAM emissions calculations. Such differences are currently not well described in the life-cycle inventory databases generally used to assess construction materials, and this area requires significant further attention in the coming years as the degree of global focus on environmental assessment of materials and processes continues to grow. A well-formulated alkali-activated concrete can often provide highly significant environmental benefits compared with a Portland cement concrete of comparable mechanical performance, which provides a strong driver for the further development and adoption of alkali activation technology on a global scale.

## 7. CONCLUSIONS

Alkali-activated binder systems, including the subclass of materials known as geopolymers, offer a high-volume, affordable, low-CO<sub>2</sub> alternative to Portland cement in a wide range of important infrastructure applications. The availability of a broader range of cementing binders is essential in enabling future society to meet its infrastructure needs while minimizing the adverse impact of such progress on the global environment. There is an imminent need to move away from a one-size-fits-all solution based on Portland cement as the binder in almost all concretes to a situation in which fit-for-purpose materials are selected on the basis of technical and environmental performance to suit each application. Alkali-activated binders will not be the only solution to this problem but will certainly form a key component of a solution toolkit, whereby a wide range of binder chemistries will be utilized in the most appropriate applications to provide the continued development of the built environment that is needed in both developed and developing nations worldwide.

In studies of any cementing binder system, and particularly of alkali-activated binders, further detailed scientific and chemical insight is needed before these materials can be fully understood from the atomic scale up to the macroscale. These materials are heterogeneous on every length scale from nanometers to centimeters, are crystallographically disordered, are multiphase, and are formed from precursors that are themselves often difficult to characterize (for example, fly ash). Many physicochemical details of these challenging and intriguing materials systems require further elucidation through the application of both top-down (macroscale and mesoscale characterization) and bottom-up (computational materials design) approaches. Thus, there is scope for significant scientific advances to be made in this field, offering the potential for a real impact on societal infrastructure development in parallel with environmental sustainability.

### FUTURE ISSUES

The scientific and engineering advances described in this review have brought alkali activation technology to the point at which successful commercial-scale deployment is taking place in many parts of the world, and research activity in this field is both widespread and intensive in the academic and commercial spheres. Nonetheless, a number of key issues require further attention from the scientific and engineering community.

1. Can we accurately describe the gel chemistry relationships in blended high-calcium/low-calcium alkali-activated gel binder systems? How can we achieve the necessary level of chemical and nanostructural characterization of these materials, using existing or new laboratory and beamline tools?
2. How can we develop the admixtures needed to control the rheology and reaction kinetics of AAMs at an early age, particularly given the chemically challenging environments (high pH, high ionic concentrations) within which these admixtures must act?

3. How can quality control be ensured in large-scale production of a material that is derived from intrinsically variable wastes or by-products? Can we relate some of this variability to the content of elements such as iron, sulfur, and magnesium that have often been assumed to be of secondary importance when compared with the main gel-forming species, but that seem to play a significant role in determining the phase assemblages present in hardened alkali-activated binders?
4. How can we obtain an accurate and representative measure of the degree of reaction in an alkali-activated binder containing fly ash and/or metakaolin? More fundamentally, what is a meaningful way to define the extent of reaction of a highly heterogeneous material such as fly ash?
5. How can we validate the life-cycle inventory databases used to assess the environmental footprint of construction materials, with a view toward enabling region-specific or site-specific life-cycle-impact calculations?
6. What are the expected service life and durability performance of an alkali-activated concrete, and how can these best be assessed and predicted on the basis of laboratory testing when most of the tests used have been designed and validated specifically for Portland cement concretes?
7. How can such a diverse group of binders be covered appropriately by regulatory standards to protect both producers and end users?

## DISCLOSURE STATEMENT

The authors are not aware of any affiliations, memberships, funding, or financial holdings that might be perceived as affecting the objectivity of this review.

## ACKNOWLEDGMENTS

We thank the colleagues who have supported and collaborated in our research for many years, in particular Professors Jannie van Deventer (University of Melbourne, Australia) and Ruby Mejía de Gutiérrez (Universidad del Valle, Colombia), who introduced us to the science and engineering of AAMs. We thank the researchers who have inspired the concepts and ideas presented in this review through journal and conference publications and through informal discussions. Lastly, we thank the funding bodies that have supported our research over the past decade, in particular the Australian Research Council and Colciencias, as well as numerous providers of travel grants and instrument/beamline access time.

## LITERATURE CITED

1. Aïtcin P-C. 2000. Cements of yesterday and today: concrete of tomorrow. *Cem. Concr. Res.* 30:1349–59
2. Hewlett PC. 1998. *Lea's Chemistry of Cement and Concrete*. Oxford, UK: Elsevier. 1,057 pp. 4th ed.
3. Scrivener KL, Kirkpatrick RJ. 2008. Innovation in use and research on cementitious material. *Cem. Concr. Res.* 38:128–36
4. Olivier JGJ, Janssens-Maenhout G, Peters JAHW. 2012. *Trends in global CO<sub>2</sub> emissions; 2012 report*. Rep., PBL Neth. Environ. Assess. Agency, The Hague
5. Gartner E. 2004. Industrially interesting approaches to “low-CO<sub>2</sub>” cements. *Cem. Concr. Res.* 34:1489–98

6. Taylor M, Tam C, Gielen D. 2006. *Energy efficiency and CO<sub>2</sub> emissions from the global cement industry*. Presented at Workshop, Energy Efficiency and CO<sub>2</sub> Emission Reduction Potentials and Policies, Int. Energy Agency, Paris, Sept. 4–5
7. Provis JL, van Deventer JSJ, eds. 2014. *Alkali-Activated Materials: State-of-the-Art Report, RILEM TC 224-AM*. Dordrecht, Neth.: RILEM/Springer
8. Davidovits J. 2008. *Geopolymer Chemistry and Applications*. Saint-Quentin, Fr.: Inst. Géopolym. 592 pp.
9. van Deventer JSJ, Provis JL, Duxson P. 2012. Technical and commercial progress in the adoption of geopolymer cement. *Miner. Eng.* 29:89–104
10. Juenger MCG, Winnefeld F, Provis JL, Ideker J. 2011. Advances in alternative cementitious binders. *Cem. Concr. Res.* 41:1232–43
11. McLellan BC, Williams RP, Lay J, van Riessen A, Corder GD. 2011. Costs and carbon emissions for geopolymer pastes in comparison to ordinary Portland cement. *J. Clean. Prod.* 19:1080–90
12. Habert G, d’Espinose de Lacaillerie JB, Roussel N. 2011. An environmental evaluation of geopolymer based concrete production: reviewing current research trends. *J. Clean. Prod.* 19:1229–38
13. Lothenbach B, Scrivener K, Hooton RD. 2011. Supplementary cementitious materials. *Cem. Concr. Res.* 41:1244–56
14. Sprung S. 2000. Cement. In *Ullmann’s Encyclopedia of Industrial Chemistry*. Wiley-VCH; doi:10.1002/14356007.a05\_489.pub2
15. Davis RE, Carlson RW, Kelly JW, Davis HE. 1937. Properties of cements and concretes containing fly ash. *J. Am. Concr. Inst.* 33:577–612
16. Kühn H. 1908. *Slag cement and process of making the same*. US Patent 900,939
17. Purdon AO. 1940. The action of alkalis on blast-furnace slag. *J. Soc. Chem. Ind. Trans. Commun.* 59:191–202
18. Buchwald A, Vanooteghem M, Gruyaert E, Hilbig H, De Belie N. 2014. Purdocement: application of alkali-activated slag cement in Belgium in the 1950s. *Mater. Struct.* In press; doi:10.1617/s11527-013-0200-8
19. Glukhovskiy VD. 1959. *Gruntosilikaty [Soil Silicates]*. Kiev: Gosstroyizdat. 154 pp.
20. Shi C, Krivenko PV, Roy DM. 2006. *Alkali-Activated Cements and Concretes*. Abingdon, UK: Taylor & Francis. 376 pp.
21. Häkkinen T. 1987. Durability of alkali-activated slag concrete. *Nord. Concr. Res.* 6:81–94
22. Wang SD. 1991. Review of recent research on alkali-activated concrete in China. *Mag. Concr. Res.* 43:29–35
23. Davidovits J. 1982. The need to create a new technical language for the transfer of basic scientific information. In *Transfer and Exploitation of Scientific and Technical Information, EUR 7716*, Proc. Symp. held by Commission of the European Communities, Directorate-General Information Market and Innovation, Luxembourg, June 10–12, 1981, pp. 316–20
24. Davidovits J. 1991. Geopolymers—inorganic polymeric new materials. *J. Therm. Anal.* 37:1633–56
25. Wastiels J, Wu X, Faiguet S, Patfoort G. 1994. Mineral polymer based on fly ash. *J. Resour. Manag. Technol.* 22:135–41
26. Blaakmeer J. 1994. Diabind: an alkali-activated slag fly ash binder for acid-resistant concrete. *Adv. Cem. Based Mater.* 1:275–76
27. Duxson P, Provis JL, Lukey GC, van Deventer JSJ. 2007. The role of inorganic polymer technology in the development of “green concrete.” *Cem. Concr. Res.* 37:1590–97
28. Provis JL. 2009. Activating solution chemistry for geopolymers. See Ref. 147, pp. 50–71
29. Wiedema B. 2008. Avoiding co-product allocation in life-cycle assessment. *J. Ind. Ecol.* 4:11–33
30. Criado M, Palomo A, Fernández-Jiménez A. 2005. Alkali activation of fly ashes. Part 1. Effect of curing conditions on the carbonation of the reaction products. *Fuel* 84:2048–54
31. Shi C. 1996. Strength, pore structure and permeability of alkali-activated slag mortars. *Cem. Concr. Res.* 26:1789–99
32. Najafi Kani E, Allahverdi A, Provis JL. 2012. Efflorescence control in geopolymer binders based on natural pozzolan. *Cem. Concr. Compos.* 34:25–33
33. Provis JL, Yong CZ, Duxson P, van Deventer JSJ. 2009. Correlating mechanical and thermal properties of sodium silicate–fly ash geopolymers. *Colloids Surf. A* 336:57–63

34. Knight CTG, Balec RJ, Kinrade SD. 2007. The structure of silicate anions in aqueous alkaline solutions. *Angew. Chem. Int. Ed.* 46:8148–52
35. Provis JL, Duxson P, Lukey GC, Separovic F, Kriven WM, van Deventer JSJ. 2005. Modeling speciation in highly concentrated alkaline silicate solutions. *Ind. Eng. Chem. Res.* 44:8899–908
36. Provis JL, van Deventer JSJ. 2007. Geopolymerisation kinetics. 2. Reaction kinetic modelling. *Chem. Eng. Sci.* 62:2318–29
37. Vail JG. 1952. *Soluble Silicates: Their Properties and Uses*. New York: Reinhold
38. Allen AJ, Thomas JJ, Jennings HM. 2007. Composition and density of nanoscale calcium–silicate–hydrate in cement. *Nat. Mater.* 6:311–16
39. Taylor R, Richardson IG, Brydson RMD. 2010. Composition and microstructure of 20-year-old ordinary Portland cement-ground granulated blast-furnace slag blends containing 0 to 100% slag. *Cem. Concr. Res.* 40:971–83
40. Wang S-D, Pu X-C, Scrivener KL, Pratt PL. 1995. Alkali-activated slag cement and concrete: a review of properties and problems. *Adv. Cem. Res.* 7:93–102
41. Krivenko PV. 1994. *Alkaline cements*. Presented at Proc. Int. Conf. Alkaline Cem. Concr., 1st, Kiev, Ukraine
42. Puertas F. 1995. Cementos de escoria activados alcalinamente: situación actual y perspectivas de futuro. *Mater. Constr.* 45:53–64
43. Provis JL, Myers RJ, White CE, Rose V, van Deventer JSJ. 2012. X-ray microtomography shows pore structure and tortuosity in alkali-activated binders. *Cem. Concr. Res.* 42:855–64
44. Fernández-Jiménez A, Palomo JG, Puertas F. 1999. Alkali-activated slag mortars. Mechanical strength behaviour. *Cem. Concr. Res.* 29:1313–21
45. Wang SD, Scrivener KL, Pratt PL. 1994. Factors affecting the strength of alkali-activated slag. *Cem. Concr. Res.* 24:1033–43
46. Fernández-Jiménez A, Puertas F, Sobrados I, Sanz J. 2003. Structure of calcium silicate hydrates formed in alkaline-activated slag: influence of the type of alkaline activator. *J. Am. Ceram. Soc.* 86:1389–94
47. Brough AR, Atkinson A. 2002. Sodium silicate-based, alkali-activated slag mortars. Part I. Strength, hydration and microstructure. *Cem. Concr. Res.* 32:865–79
48. Myers RJ, Bernal SA, San Nicolas R, Provis JL. 2013. Generalized structural description of calcium-sodium aluminosilicate hydrate gels: the crosslinked substituted tobermorite model. *Langmuir* 29:5294–306
49. Richardson IG, Brough AR, Groves GW, Dobson CM. 1994. The characterization of hardened alkali-activated blast-furnace slag pastes and the nature of the calcium silicate hydrate (C-S-H) paste. *Cem. Concr. Res.* 24:813–29
50. Puertas F, Palacios M, Manzano H, Dolado JS, Rico A, Rodríguez J. 2011. A model for the C-A-S-H gel formed in alkali-activated slag cements. *J. Eur. Ceram. Soc.* 31:2043–56
51. Escalante-García J, Fuentes AF, Gorokhovskiy A, Fraire-Luna PE, Mendoza-Suarez G. 2003. Hydration products and reactivity of blast-furnace slag activated by various alkalis. *J. Am. Ceram. Soc.* 86:2148–53
52. Skinner LB, Chae SR, Benmore CJ, Wenk HR, Monteiro PJM. 2010. Nanostructure of calcium silicate hydrates in cements. *Phys. Rev. Lett.* 104:195502
53. Richardson IG, Brough AR, Brydson R, Groves GW, Dobson CM. 1993. Location of aluminum in substituted calcium silicate hydrate (C-S-H) gels as determined by <sup>29</sup>Si and <sup>27</sup>Al NMR and EELS. *J. Am. Ceram. Soc.* 76:2285–88
54. Sun GK, Young JF, Kirkpatrick RJ. 2006. The role of Al in C-S-H: NMR, XRD, and compositional results for precipitated samples. *Cem. Concr. Res.* 36:18–29
55. Taylor R, Richardson IG, Brydson RMD. 2007. Nature of C-S-H in 20 year old neat ordinary Portland cement and 10% Portland cement–90% ground granulated blast furnace slag pastes. *Adv. Appl. Ceram.* 106:294–301
56. Richardson IG. 2008. The calcium silicate hydrates. *Cem. Concr. Res.* 38:137–58
57. Bernal SA, Provis JL, Walkley B, San Nicolas R, Gehman JD, et al. 2013. Gel nanostructure in alkali-activated binders based on slag and fly ash, and effects of accelerated carbonation. *Cem. Concr. Res.* 53:127–44

58. Chen W, Brouwers H. 2007. The hydration of slag. Part 1. Reaction models for alkali-activated slag. *J. Mater. Sci.* 42:428–43
59. Lothenbach B, Gruskovnjak A. 2007. Hydration of alkali-activated slag: thermodynamic modelling. *Adv. Cem. Res.* 19:81–92
60. Wang SD, Scrivener KL. 1995. Hydration products of alkali-activated slag cement. *Cem. Concr. Res.* 25:561–71
61. Bonk F, Schneider J, Cincotto MA, Panepucci H. 2003. Characterization by multinuclear high-resolution NMR of hydration products in activated blast-furnace slag pastes. *J. Am. Ceram. Soc.* 86:1712–19
62. Brown PW. 1990. The system  $\text{Na}_2\text{O}-\text{CaO}-\text{SiO}_2-\text{H}_2\text{O}$ . *J. Am. Ceram. Soc.* 73:3457–561
63. Hong S-Y, Glasser FP. 1999. Alkali binding in cement pastes. Part I. The C-S-H phase. *Cem. Concr. Res.* 29:1893–903
64. Stade H. 1989. On the reaction of C-S-H(di, poly) with alkali hydroxides. *Cem. Concr. Res.* 19:802–10
65. Shi C. 2003. *On the state and role of alkalis during the activation of alkali-activated slag cement*. Presented at Int. Congr. Chem. Cem., 11th, Durban, South Africa
66. García Lodeiro I, Macphée DE, Palomo A, Fernández-Jiménez A. 2009. Effect of alkalis on fresh C-S-H gels. FTIR analysis. *Cem. Concr. Res.* 39:147–53
67. Jackson MD, Moon J, Gotti E, Taylor R, Chae SR, et al. 2013. Material and elastic properties of Al-tobermorite in ancient Roman seawater concrete. *J. Am. Ceram. Soc.* 96:2598–606
68. Ilyin VP. 1994. *Durability of materials based on slag-alkaline binders*. Presented at Proc. Int. Conf. Alkaline Cem. Concr., 1st, Kiev, Ukraine
69. Xu H, Provis JL, van Deventer JSJ, Krivenko PV. 2008. Characterization of aged slag concretes. *ACI Mater. J.* 105:131–39
70. Bernal SA, San Nicolas R, Provis JL, Mejía de Gutiérrez R, van Deventer JSJ. 2014. Natural carbonation of aged alkali-activated slag concretes. *Mater. Struct.* 47:693–707. doi:10.1617/s11527-013-0089-2
71. Talling B, Brandstetr J. 1989. *Present state and future of alkali-activated slag concretes*. Presented at Int. Conf., Fly Ash, Silica Fume, Slag and Natural Pozzolans in Concrete, 3rd, ACI SP114, Trondheim, Nor.
72. Glasser FP. 2001. Mineralogical aspects of cement in radioactive waste disposal. *Miner. Mag.* 65: 621–33
73. Ben Haha M, Lothenbach B, Le Saout G, Winnefeld F. 2011. Influence of slag chemistry on the hydration of alkali-activated blast-furnace slag. Part I. Effect of MgO. *Cem. Concr. Res.* 41:955–63
74. Douglas E, Brandstetr J. 1990. A preliminary study on the alkali activation of ground granulated blast-furnace slag. *Cem. Concr. Res.* 20:746–56
75. Bernal SA, San Nicolas R, Myers RJ, Mejía de Gutiérrez R, Puertas F, et al. 2014. Slag chemistry controls phase evolution and structural changes induced by accelerated carbonation in alkali-activated binders. *Cem. Concr. Res.* 57:33–43
76. Mills SJ, Christy AG, Génin JMR, Kameda T, Colombo F. 2012. Nomenclature of the hydrotalcite supergroup: natural layered double hydroxides. *Miner. Mag.* 76:1289–336
77. Ben Haha M, Lothenbach B, Le Saout G, Winnefeld F. 2012. Influence of slag chemistry on the hydration of alkali-activated blast-furnace slag. Part II. Effect of  $\text{Al}_2\text{O}_3$ . *Cem. Concr. Res.* 42:74–83
78. Oh JE, Clark SM, Monteiro PJM. 2011. Does the Al substitution in C-S-H(I) change its mechanical property? *Cem. Concr. Res.* 41:102–6
79. Provis JL, Lukey GC, van Deventer JSJ. 2005. Do geopolymers actually contain nanocrystalline zeolites? A reexamination of existing results. *Chem. Mater.* 17:3075–85
80. Duxson P, Provis JL, Lukey GC, Separovic F, van Deventer JSJ. 2005.  $^{29}\text{Si}$  NMR study of structural ordering in aluminosilicate geopolymer gels. *Langmuir* 21:3028–36
81. Glukhovskiy VD. 1994. *Ancient, modern and future concretes*. Presented at Proc. Int. Conf. Alkaline Cem. Concr., 1st, Kiev, Ukraine
82. Bell JL, Sarin P, Provis JL, Haggerty RP, Driemeyer PE, et al. 2008. Atomic structure of a cesium aluminosilicate geopolymer: a pair distribution function study. *Chem. Mater.* 20:4768–76
83. White CE, Provis JL, Proffen T, van Deventer JSJ. 2010. The effects of temperature on the local structure of metakaolin-based geopolymer binder: a neutron pair distribution function investigation. *J. Am. Ceram. Soc.* 93:3486–92

84. Zhang Z, Wang H, Provis JL, Bullen F, Reid A, Zhu Y. 2012. Quantitative kinetic and structural analysis of geopolymers. Part I. The activation of metakaolin with sodium hydroxide. *Thermochim. Acta* 539:23–33
85. Bortnovsky O, Dědeček J, Tvarůžková Z, Sobalík Z, Šubrt J. 2008. Metal ions as probes for characterization of geopolymer materials. *J. Am. Ceram. Soc.* 91:3052–57
86. Fernández-Jiménez A, Monzó M, Vicent M, Barba A, Palomo A. 2008. Alkaline activation of metakaolin-fly ash mixtures: obtain of zeoceramics and zeocements. *Microporous Mesoporous Mater.* 108:41–49
87. Brindley GW, Nakahira M. 1959. The kaolinite-mullite reaction series. 2. Metakaolin. *J. Am. Ceram. Soc.* 42:314–18
88. Granizo ML, Blanco-Varela MT, Palomo A. 2000. Influence of the starting kaolin on alkali-activated materials based on metakaolin. Study of the reaction parameters by isothermal conduction calorimetry. *J. Mater. Sci.* 35:6309–15
89. Lee S, Kim YJ, Moon HS. 2003. Energy-filtering transmission electron microscopy (EF-TEM) study of a modulated structure in metakaolinite, represented by a 14 Å modulation. *J. Am. Ceram. Soc.* 86:174–76
90. White CE, Provis JL, Proffen T, van Deventer JSJ. 2012. Molecular mechanisms responsible for the structural changes occurring during geopolymerization: multiscale simulation. *AICbE J.* 58:2241–53
91. White CE, Provis JL, Proffen T, Riley DP, van Deventer JSJ. 2010. Density functional modeling of the local structure of kaolinite subjected to thermal dehydroxylation. *J. Phys. Chem. A* 114:4998–96
92. Palomo A, Alonso S, Fernández-Jiménez A, Sobrados I, Sanz J. 2004. Alkaline activation of fly ashes: NMR study of the reaction products. *J. Am. Ceram. Soc.* 87:1141–45
93. Duxson P, Lukey GC, Separovic F, van Deventer JSJ. 2005. The effect of alkali cations on aluminum incorporation in geopolymeric gels. *Ind. Eng. Chem. Res.* 44:832–39
94. Duxson P, Lukey GC, van Deventer JSJ. 2007. Characteristics of thermal shrinkage and weight loss in Na-geopolymer derived from metakaolin. *J. Mater. Sci.* 42:3044–54
95. Vance ER, Hadley JH, Hsu FH, Drabarek E. 2008. Positron annihilation lifetime spectra in a metakaolin-based geopolymer. *J. Am. Ceram. Soc.* 91:664–66
96. Baerlocher C, Meier WM, Olson DH. 2001. *Atlas of Zeolite Framework Types*. Amsterdam: Elsevier. 5th ed.
97. Provis JL, Yong SL, Duxson P. 2009. Nanostructure/microstructure of metakaolin geopolymers. See Ref. 147, pp. 72–88
98. Rowles M, O'Connor B. 2003. Chemical optimisation of the compressive strength of aluminosilicate geopolymers synthesised by sodium silicate activation of metakaolinite. *J. Mater. Chem.* 13:1161–65
99. Duxson P, Provis JL, Lukey GC, Mallicoat SW, Kriven WM, van Deventer JSJ. 2005. Understanding the relationship between geopolymer composition, microstructure and mechanical properties. *Colloids Surf. A* 269:47–58
100. Fernández-Jiménez A, Palomo A, Criado M. 2005. Microstructure development of alkali-activated fly ash cement: a descriptive model. *Cem. Concr. Res.* 35:1204–9
101. Criado M, Fernández-Jiménez A, de la Torre AG, Aranda MAG, Palomo A. 2007. An XRD study of the effect of the SiO<sub>2</sub>/Na<sub>2</sub>O ratio on the alkali activation of fly ash. *Cem. Concr. Res.* 37:671–79
102. Lloyd RR, Provis JL, Smeaton KJ, van Deventer JSJ. 2009. Spatial distribution of pores in fly ash-based inorganic polymer gels visualised by Wood's metal intrusion. *Microporous Mesoporous Mater.* 126:32–39
103. van Jaarsveld JGS, van Deventer JSJ, Lukey GC. 2004. A comparative study of kaolinite versus metakaolinite in fly ash based geopolymers containing immobilized metals. *Chem. Eng. Commun.* 191:531–49
104. Bernal SA, Rodríguez ED, Mejía de Gutierrez R, Gordillo M, Provis JL. 2011. Mechanical and thermal characterisation of geopolymers based on silicate-activated metakaolin/slag blends. *J. Mater. Sci.* 46:5477–86
105. Bernal SA, Provis JL, Mejía de Gutierrez R, Rose V. 2011. Evolution of binder structure in sodium silicate-activated slag-metakaolin blends. *Cem. Concr. Compos.* 33:46–54
106. Pacheco-Torgal F, Castro-Gomes JP, Jalali S. 2008. Investigations on mix design of tungsten mine waste geopolymeric binder. *Constr. Build. Mater.* 22:1939–49
107. Buchwald A, Hohmann M, Posern K, Brendler E. 2009. The suitability of thermally activated illite/smectite clay as raw material for geopolymer binders. *Appl. Clay Sci.* 46:300–4
108. MacKenzie KJD, Komphanchai S, Vagana R. 2008. Formation of inorganic polymers (geopolymers) from 2:1 layer lattice aluminosilicates. *J. Eur. Ceram. Soc.* 28:177–81

109. Wang L, Zhang M, Redfern SAT, Zhang Z. 2002. Dehydroxylation and transformations of the 2:1 phyllosilicate pyrophyllite at elevated temperatures: an infrared spectroscopic study. *Clays Clay Miner.* 50:272–83
110. MacKenzie KJD, Brew DRM, Fletcher RA, Vagana R. 2007. Formation of aluminosilicate geopolymers from 1:1 layer-lattice minerals pre-treated by various methods: a comparative study. *J. Mater. Sci.* 42:4667–74
111. van Deventer JSJ, Provis JL, Duxson P, Lukey GC. 2007. Reaction mechanisms in the geopolymeric conversion of inorganic waste to useful products. *J. Hazard. Mater.* A139:506–13
112. Criado M, Fernández-Jiménez A, Palomo A, Sobrados I, Sanz J. 2008. Alkali activation of fly ash. Effect of the SiO<sub>2</sub>/Na<sub>2</sub>O ratio. Part II. <sup>29</sup>Si MAS-NMR survey. *Microporous Mesoporous Mater.* 109:525–34
113. Ruiz-Santaquiteria C, Skibsted J, Fernández-Jiménez A, Palomo A. 2012. Alkaline solution/binder ratio as a determining factor in the alkaline activation of aluminosilicates. *Cem. Concr. Res.* 42:1242–51
114. Oh JE, Monteiro PJM, Jun SS, Choi S, Clark SM. 2010. The evolution of strength and crystalline phases for alkali-activated ground blast furnace slag and fly ash-based geopolymers. *Cem. Concr. Res.* 40:189–96
115. Rees CA, Provis JL, Lukey GC, van Deventer JSJ. 2007. Attenuated total reflectance Fourier transform infrared analysis of fly ash geopolymer gel aging. *Langmuir* 23:8170–79
116. Lee WKW, van Deventer JSJ. 2003. Use of infrared spectroscopy to study geopolymerization of heterogeneous amorphous aluminosilicates. *Langmuir* 19:8726–34
117. Fernández-Jiménez A, Palomo A. 2005. Mid-infrared spectroscopic studies of alkali-activated fly ash structure. *Microporous Mesoporous Mater.* 86:207–14
118. White CE, Provis JL, Kearley GJ, Riley DP, van Deventer JSJ. 2011. Density functional modelling of silicate and aluminosilicate dimerisation solution chemistry. *Dalton Trans.* 40:1348–55
119. Rees CA, Provis JL, Lukey GC, van Deventer JSJ. 2007. In situ ATR-FTIR study of the early stages of fly ash geopolymer gel formation. *Langmuir* 23:9076–82
120. Hajimohammadi A, Provis JL, van Deventer JSJ. 2010. The effect of alumina release rate on the mechanism of geopolymer gel formation. *Chem. Mater.* 22:5199–208
121. Provis JL, van Deventer JSJ. 2007. Direct measurement of the kinetics of geopolymerisation by in-situ energy dispersive X-ray diffractometry. *J. Mater. Sci.* 42:2974–81
122. Favier A, Habert G, d'Espinose de Lacaillerie JB, Roussel N. 2013. Mechanical properties and compositional heterogeneities of fresh geopolymer pastes. *Cem. Concr. Res.* 48:9–16
123. White CE, Provis JL, Llobet A, Proffen T, van Deventer JSJ. 2011. Evolution of local structure in geopolymer gels: an in-situ neutron pair distribution function analysis. *J. Am. Ceram. Soc.* 94:3532–39
124. Winnefeld F, Leemann A, Lucuk M, Svoboda P, Neuroth M. 2010. Assessment of phase formation in alkali activated low and high calcium fly ashes in building materials. *Constr. Build. Mater.* 24:1086–93
125. Lloyd RR, Provis JL, van Deventer JSJ. 2010. Pore solution composition and alkali diffusion in inorganic polymer cement. *Cem. Concr. Res.* 40:1386–92
126. Duxson P, Provis JL. 2008. Designing precursors for geopolymer cements. *J. Am. Ceram. Soc.* 91:3864–69
127. Diaz-Loya EI, Allouche EN, Vaidya S. 2011. Mechanical properties of fly-ash-based geopolymer concrete. *ACI Mater. J.* 108:300–6
128. Fernández-Jiménez A, de la Torre AG, Palomo A, López-Olmo G, Alonso MM, Aranda MAG. 2006. Quantitative determination of phases in the alkali activation of fly ash. Part I. Potential ash reactivity. *Fuel* 85:625–34
129. Ben Haha M, De Weerd K, Lothenbach B. 2010. Quantification of the degree of reaction of fly ash. *Cem. Concr. Res.* 40:1620–29
130. Puertas F, Martínez-Ramírez S, Alonso S, Vázquez E. 2000. Alkali-activated fly ash/slag cement. Strength behaviour and hydration products. *Cem. Concr. Res.* 30:1625–32
131. Puertas F, Fernández-Jiménez A. 2003. Mineralogical and microstructural characterisation of alkali-activated fly ash/slag pastes. *Cem. Concr. Compos.* 25:287–92
132. Ismail I, Bernal SA, Provis JL, San Nicolas R, Hamdan S, van Deventer JSJ. 2014. Modification of phase evolution in alkali-activated blast furnace slag by the incorporation of fly ash. *Cem. Concr. Compos.* 45:125–35

133. Ismail I, Bernal SA, Provis JL, San Nicolas R, Brice DG, et al. 2013. Influence of fly ash on the water and chloride permeability of alkali-activated slag mortars and concretes. *Constr. Build. Mater.* 48:1187–201
134. Yip CK, Lukey GC, van Deventer JSJ. 2005. The coexistence of geopolymeric gel and calcium silicate hydrate at the early stage of alkaline activation. *Cem. Concr. Res.* 35:1688–97
135. Alonso S, Palomo A. 2001. Alkaline activation of metakaolin and calcium hydroxide mixtures: influence of temperature, activator concentration and solids ratio. *Mater. Lett.* 47:55–62
136. Donatello S, Fernández-Jiménez A, Palomo A. 2013. Very high volume fly ash cements. Early age hydration study using  $\text{Na}_2\text{SO}_4$  as an activator. *J. Am. Ceram. Soc.* 96:900–6
137. Bernal S, Skibsted J, Herfort D. 2011. *Hybrid binders based on alkali sulfate-activated Portland clinker and metakaolin*. Presented at Int. Congr. Chem. Cem., 13th, Madrid
138. Granizo ML, Alonso S, Blanco-Varela MT, Palomo A. 2002. Alkaline activation of metakaolin: effect of calcium hydroxide in the products of reaction. *J. Am. Ceram. Soc.* 85:225–31
139. Yip CK, van Deventer JSJ. 2003. Microanalysis of calcium silicate hydrate gel formed within a geopolymeric binder. *J. Mater. Sci.* 38:3851–60
140. Buchwald A, Hilbig H, Kaps C. 2007. Alkali-activated metakaolin-slag blends—performance and structure in dependence on their composition. *J. Mater. Sci.* 42:3024–32
141. Dombrowski K, Buchwald A, Weil M. 2007. The influence of calcium content on the structure and thermal performance of fly ash based geopolymers. *J. Mater. Sci.* 42:3033–43
142. Smith MA, Osborne GJ. 1977. Slag/fly ash cements. *World Cem. Technol.* 1:223–33
143. Lloyd RR. 2008. *The Durability of Inorganic Polymer Cements*. PhD thesis. Univ. Melbourne
144. Li Z, Liu S. 2007. Influence of slag as additive on compressive strength of fly ash-based geopolymer. *J. Mater. Civil Eng.* 19:470–74
145. García-Lodeiro I, Palomo A, Fernández-Jiménez A, Macphee DE. 2011. Compatibility studies between N-A-S-H and C-A-S-H gels. Study in the ternary diagram  $\text{Na}_2\text{O-CaO-Al}_2\text{O}_3\text{-SiO}_2\text{-H}_2\text{O}$ . *Cem. Concr. Res.* 41:923–31
146. Fawer M, Concannon M, Rieber W. 1999. Life cycle inventories for the production of sodium silicates. *Int. J. Life Cycle Assess.* 4:207–12
147. Provis JL, van Deventer JSJ, eds. 2009. *Geopolymers: Structure, Processing, Properties and Industrial Applications*. Cambridge, UK: Woodhead

---

## RELATED RESOURCES

1. Bernal SA, Mejía de Gutiérrez R, Pedraza AL, Provis JL, Rodríguez ED, Delvasto S. 2011. Effect of binder content on the performance of alkali-activated slag concretes. *Cem. Concr. Res.* 41:1–8
2. Bernal SA, Provis JL, Rose V, Mejía de Gutiérrez R. 2013. High-resolution X-ray diffraction and fluorescence microscopy characterization of alkali-activated slag-metakaolin binders. *J. Am. Ceram. Soc.* 96:1951–57
3. Damtoft JS, Lukasik J, Herfort D, Sorrentino D, Gartner E. 2008. Sustainable development and climate change initiatives. *Cem. Concr. Res.* 38:115–27
4. Duxson P, Fernández-Jiménez A, Provis JL, Lukey GC, Palomo A, van Deventer JSJ. 2007. Geopolymer technology: the current state of the art. *J. Mater. Sci.* 42:2917–33
5. Gartner EM, Macphee DE. 2011. A physico-chemical basis for novel cementitious binders. *Cem. Concr. Res.* 41:736–49
6. Moseson AJ, Moseson DE, Barsoum MW. 2012. High volume limestone alkali-activated cement developed by design of experiment. *Cem. Concr. Compos.* 34:328–36
7. Provis JL, Duxson P, van Deventer JSJ. 2010. The role of particle technology in developing sustainable construction materials. *Adv. Powder Technol.* 21:2–7

8. Provis JL, Hajimohammadi A, White CE, Bernal SA, Myers RJ, et al. 2013. Nanostructural characterization of geopolymers by advanced beamline techniques. *Cem. Concr. Compos.* 36:56–64
9. Provis JL, Rose V, Bernal SA, van Deventer JSJ. 2009. High resolution nanoprobe X-ray fluorescence characterization of heterogeneous calcium and heavy metal distributions in alkali activated fly ash. *Langmuir* 25:11897–904
10. van Deventer JSJ, Provis JL, Duxson P, Brice DG. 2010. Chemical research and climate change as drivers in the commercial adoption of alkali activated materials. *Waste Biomass Valoriz.* 1:145–55